



**UNIVERSIDAD DE INVESTIGACIÓN DE TECNOLOGÍA
EXPERIMENTAL YACHAY**

Escuela de Ciencias de la Tierra, Energía y Ambiente

**TÍTULO: Tectono-Sedimentary Evolution of the Northern Part of
the Esmeraldas-Borbón Basin (Northern Ecuadorian Forearc)**

Trabajo de integración curricular presentado como requisito para
la obtención del título de Geólogo

Autor:

Chalampunte Flores Andrés Israel

Tutor:

Emilio Carrillo, Ph.D

Co-Tutor:

Yaniel Vázquez, Ph.D

Urququí, Noviembre 2020

Urucuquí, 13 de noviembre de 2020

SECRETARÍA GENERAL
(Vicerrectorado Académico/Cancillería)
ESCUELA DE CIENCIAS DE LA TIERRA, ENERGÍA Y AMBIENTE
CARRERA DE GEOLOGÍA
ACTA DE DEFENSA No. UITEY-GEO-2020-00014-AD

A los 13 días del mes de noviembre de 2020, a las 15:00 horas, de manera virtual mediante videoconferencia, y ante el Tribunal Calificador, integrado por los docentes:

Presidente Tribunal de Defensa	Dr. ALMEIDA GONZALEZ, RAFAEL VLADIMIR , Ph.D.
Miembro No Tutor	Dra. FOSTER ANNA ELIZABETH , Ph.D.
Tutor	Dr. CARRILLO ALVAREZ, EMILIO , Ph.D.

El(la) señor(ita) estudiante **CHALAMPUENTE FLORES, ANDRES ISRAEL**, con cédula de identidad No. **1003833280**, de la **ESCUELA DE CIENCIAS DE LA TIERRA, ENERGÍA Y AMBIENTE**, de la Carrera de **GEOLOGÍA**, aprobada por el Consejo de Educación Superior (CES), mediante Resolución **RPC-SE-10-No.031-2016**, realiza a través de videoconferencia, la sustentación de su trabajo de titulación denominado: **TECTONO-SEDIMENTARY EVOLUTION OF THE NORTHERN PART OF THE ESMERALDAS-BORBÓN BASIN**, previa a la obtención del título de **GEÓLOGO/A**.

El citado trabajo de titulación, fue debidamente aprobado por el(los) docente(s):

Tutor	Dr. CARRILLO ALVAREZ, EMILIO , Ph.D.
--------------	--------------------------------------

Y recibió las observaciones de los otros miembros del Tribunal Calificador, las mismas que han sido incorporadas por el(la) estudiante.

Previamente cumplidos los requisitos legales y reglamentarios, el trabajo de titulación fue sustentado por el(la) estudiante y examinado por los miembros del Tribunal Calificador. Escuchada la sustentación del trabajo de titulación a través de videoconferencia, que integró la exposición de el(la) estudiante sobre el contenido de la misma y las preguntas formuladas por los miembros del Tribunal, se califica la sustentación del trabajo de titulación con las siguientes calificaciones:


Tipo	Docente	Calificación
Tutor	Dr. CARRILLO ALVAREZ, EMILIO , Ph.D.	9,3
Miembro Tribunal De Defensa	Dra. FOSTER ANNA ELIZABETH , Ph.D.	9,1
Presidente Tribunal De Defensa	Dr. ALMEIDA GONZALEZ, RAFAEL VLADIMIR , Ph.D.	8,9

Lo que da un promedio de: **9.1 (Nueve punto Uno)**, sobre 10 (diez), equivalente a: **APROBADO**

Para constancia de lo actuado, firman los miembros del Tribunal Calificador, el/la estudiante y el/la secretario ad-hoc.

Certifico que en cumplimiento del Decreto Ejecutivo 1017 de 16 de marzo de 2020, la defensa de trabajo de titulación (o examen de grado modalidad teórico práctica) se realizó vía virtual, por lo que las firmas de los miembros del Tribunal de Defensa de Grado, constan en forma digital.

CHALAMPUENTE FLORES, ANDRES ISRAEL
Estudiante



RAFAEL VLADIMIR ALMEIDA GONZALEZ

Dr. ALMEIDA GONZALEZ, RAFAEL VLADIMIR , Ph.D.
Presidente Tribunal de Defensa

Digitally signed by RAFAEL VLADIMIR ALMEIDA GONZALEZ
 DN: cn=RAFAEL VLADIMIR ALMEIDA GONZALEZ, serialNumber=211020132449, ou=ENTIDAD DE CERTIFICACION DE INFORMACION, o=SECURITY DATA S.A. 2, c=EC
 Date: 2020.11.13 16:27:35 -05'00'

Dr. CARRILLO ALVAREZ, EMILIO , Ph.D.
Tutor

EMILIO CARRILLO ALVAREZ

Firmado digitalmente por EMILIO CARRILLO ALVAREZ
 Nombre de inscripción: CN=, c=EC, ou=BANCO CENTRAL DEL ECUADOR, ou=SECRETARIA CALIFICACIONES, INFORMATION ECORIE, L-QATO
 email=Rafael@1003833280.ec, cn=EMILIO CARRILLO ALVAREZ
 Fecha: 2020.11.13 15:48:12 -0500'

Dra. FOSTER ANNA ELIZABETH , Ph.D.
Miembro No Tutor

ANNA
ELIZABETH
FOSTER  Digitally signed by ANNA
ELIZABETH FOSTER
Date: 2020.11.14 13:08:31
-05'00'

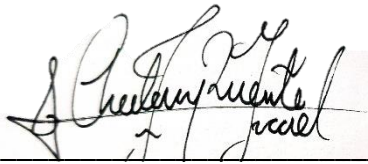
TERÁN ROSALES, ANDREA YOLANDA
Secretario Ad-hoc

ANDREA
YOLANDA
TERAN
ROSALES  Firmado digitalmente
por ANDREA YOLANDA
TERAN ROSALES
Fecha: 2020.11.13
16:21:01 -05'00'

AUTORÍA

Yo, **Andrés Israel Chalampunte Flores**, con cédula de identidad 1003833280, declaro que las ideas, juicios, valoraciones, interpretaciones, consultas bibliográficas, definiciones y conceptualizaciones expuestas en el presente trabajo; así como, los procedimientos y herramientas utilizadas en la investigación, son de absoluta responsabilidad de el/la autora (a) del trabajo de integración curricular. Así mismo, me acojo a los reglamentos internos de la Universidad de Investigación de Tecnología Experimental Yachay.

Urcuquí, noviembre 2020.

A handwritten signature in black ink, appearing to read 'Andrés Israel Chalampunte Flores', written over a horizontal line.


Andrés Israel Chalampunte Flores
CI: 1003833280

AUTORIZACIÓN DE PUBLICACIÓN

Yo, **Andrés Israel Chalampunte Flores**, con cédula de identidad 1003833280, cedo a la Universidad de Investigación de Tecnología Experimental Yachay, los derechos de publicación de la presente obra, sin que deba haber un reconocimiento económico por este concepto. Declaro además que el texto del presente trabajo de titulación no podrá ser cedido a ninguna empresa editorial para su publicación u otros fines, sin contar previamente con la autorización escrita de la Universidad.

Asimismo, autorizo a la Universidad que realice la digitalización y publicación de este trabajo de integración curricular en el repositorio virtual, de conformidad a lo dispuesto en el Art. 144 de la Ley Orgánica de Educación Superior

Urququí, noviembre 2020.

A handwritten signature in black ink, appearing to read 'Andrés Israel Chalampunte Flores', written over a horizontal line.

Andrés Israel Chalampunte Flores
CI: 1003833280

Acknowledgments

I want to dedicate my thesis work to all my family, especially to my mother Josefina Flores, and my father Héctor Chalampunte, which during my career they supported me since I decided to study in Yachay Tech. I want to recognize that they are my best inspiration to keep on in my studies, and never give up. Likewise, I want to thank my brothers and sisters, which they gave me much advice and help in the different problems throughout my career.

I am very grateful to all my professors, which they taught me many things not just about my career but also, they taught me responsibility, honesty, gratitude, and friendship. All of these to be a better person and professional. Furthermore, I am grateful to my advisor Emilio Carrillo that never let me alone during the realization of this work, and I am extremely grateful to him because he is always at any time to help me to solve any problem or doubt. Last but not least, I want to thank to my all friends. They are a very important part of my life because with them I have spent great moments in my life, and they are always there for me in good and bad times.

This thesis work is a representation of effort and perseverance since I started my studies at Yachay Tech. It is my first step, and I promise to myself never give up, always give my best, and I will keep improving. This is not the end of my career. It is the beginning of a new stage of my life.

Andrés Israel Chalampunte Flores

Resumen

La historia tectónica del Cretácico al Neógeno del margen noroeste de América del Sur, que involucra la acreción e interacciones entre las placas del Caribe y América del Sur, es compleja. En Ecuador, los estudios geoquímicos y geocronológicos han proporcionado un marco para la interpretación de las evoluciones paleotectónicas 2D. A pesar de esto, aún existe incertidumbre sobre la historia tectónica de este margen. Si bien existen algunos estudios de las cuencas de Manabí y Progreso en el antearco sur del Ecuador, faltan en la literatura estudios tectono-sedimentarios que propongan reconstrucciones paleotectónicas.

En este trabajo, utilizamos un conjunto de líneas sísmicas de la industria, combinadas con datos de pozos de la cuenca de antearco del norte de Ecuador, específicamente de la cuenca Esmeraldas-Borbón, para realizar dicho estudio. Con estos datos se realizaron mapas estructurales e isopacas para conocer la evolución tectono-sedimentaria de un área de estudio seleccionada.

Esta investigación muestra la existencia de estructuras que afectan una sucesión sincompresiva del Cretácico Tardío al Neógeno que se divide en ocho secuencias deposicionales. Además, se interpreta una evolución tectono-sedimentaria entre el Cretácico Superior y el Mioceno Inferior. Esta evolución consistió en los siguientes tres ambientes: 1) plataforma carbonatada poco profunda a profunda, Cretácico tardío a Oligoceno temprano, con dirección de flujo sureste; 2) plataforma siliciclástica poco profunda a profunda, Oligoceno temprano a tardío, con una dirección de flujo noreste; y 3) plataforma al sistema siliciclástico en abanico de aguas profundas, Oligoceno tardío a Mioceno tardío con dirección de flujo noreste.

Los resultados de este estudio son de gran relevancia para cualquier interpretación futura relacionada con las interacciones entre las placas del Caribe, Nazca y Sudamérica..

Palabras Claves: tectono-sedimentario, Cuenca Esmeraldas-Borbón, Cuenca del antearco, Ecuador.

Abstract

The Cretaceous to Neogene tectonic history of the northwestern margin of South America, involving accretion and interactions between the Caribbean and South American plates, is complex. In Ecuador, geochemical and geochronological studies have provided a framework for interpretations of 2D paleotectonic evolutions. In spite of this, there is still uncertainty regarding the tectonic history of this margin. Even though there are some studies from the Manabí and Progreso basins in the southern Ecuadorian forearc, tectono-sedimentary studies proposing paleotectonic reconstructions are missing in the literature.

In this work, we use a set of industry seismic lines, combined with well data from the northern Ecuadorian forearc basin, specifically from the Esmeraldas-Borbón Basin, to carry out such a study. With this data, structural and isopach maps were made to know the tectono-sedimentary evolution of a selected study area.

This research shows the existence of structures affecting a Late Cretaceous to Neogene syn-compressional succession which is divided in eight depositional sequences. Moreover, a tectono-sedimentary evolution is interpreted between Late Cretaceous and Early Miocene. This evolution consisted by the following three environments: 1) shallow to deep carbonate platform, Late Cretaceous to Early Oligocene, with a southeast flow direction; 2) shallow to deep siliciclastic platform, Early to Late Oligocene, with a northeastern flow direction; and 3) platform to deep sea fan siliciclastic system, Late Oligocene to Late Miocene with northeastern flow direction.

The results of this study are of great relevance for any future interpretation related to the interactions between the Caribbean, Nazca, and South American plates.

Keywords: tectono-sedimentary, Esmeraldas-Borbón Basin, forearc basin, Ecuador.

CONTENT

CHAPTER 1: INTRODUCTION	19
1.1. Background.....	19
1.2. Rationale	22
1.3. The Esmeraldas-Borbón Basin	22
1.4. Objectives.....	24
CHAPTER 2: GEOLOGICAL SETTING	25
2.1. Geological features of a forearc region	25
2.2. Regional features	25
2.3. Stratigraphy	26
2.2.1. Piñon Formation (KPñ)	29
2.2.2. Cayo Formation (KCy)	29
2.2.3. Zapallo Formation (EZp)	30
2.2.4. Playa Rica Formation (OPr)	30
2.2.5. Pambil Formation (OPm)	31
2.2.6. Viche Formation (MVh-Db)	31
2.2.7. Angostura Formation (MAG)	31
2.2.8. Ónzole Formation (MOz)	32
2.2.9. Cachabi Formation (PLB-Ch)	32
2.3. Structural Features.....	33
CHAPTER 3: DATA SET AND METHODS	35
3.1. Data set	35
3.2. Methodology	36
3.2.1. Depositional sequences and sedimentary framework	36
3.2.2. Interpretation and regional framework	37
CHAPTER 4: RESULTS	38
4.1. A Sequence	38
4.2. B Sequence	39
4.3. C Sequence	39
4.4. D Sequence	40
4.5. E Sequence	41
4.6. F Sequence	41
4.7. G Sequence	42
4.8. H Sequence	42
CHAPTER 5: DISCUSSION	50
5.1. Chronostratigraphic Relationship	50
5.2 Structural Interpretation	52
5.3. Tectono-sedimentary evolution.....	53
5.3.1. Stage 1: Late Cretaceous to Early Oligocene.....	54

5.3.2. Stage 2: Early to Late Oligocene.....	54
5.3.3. Stage 3: Late Oligocene to Late Miocene.....	54
CHAPTER 6: CONCLUSION	57
References.	58

CHAPTER 1: INTRODUCTION

1.1. Background

The Cretaceous to Neogene tectonic history of the northwestern margin of South America, involving accretions and interactions between the Caribbean and South American plates, is complex (Daly, 1989; Kerr et al., 2002; Jaillard et al., 2007). During this history, the margin of northern South America was deformed synchronously to fragmentation of the Caribbean Plate (Mora et al., 2017; Luzieux, 2006). Likewise, based on geochronological and geochemical analysis of mafic oceanic rocks from the central part of the northwestern Andean margin, documented in previous studies (Vallejo et al., 2019; Kerr et al., 2002; Vallejo et al., 2006; Jaillard et al., 2007), it is interpreted that the basement of this margin correlates with the Caribbean and Central American regions (Fig. 1).

The formation of the forearc region of Ecuador is related to the collision of the Caribbean Plateau beneath the South America Plate during the Late Cretaceous (Luzieux, 2006). In Colombia, tectonostratigraphic analysis in forearc basins (e.g., Lower Magdalena Valley, San Jacinto, and Cesar-Ranchería basins) (e.g., Mora et al., 2017; Mantilla et al., 2009; Bernal-Olaya et al., 2015) record a collision of the Caribbean Plate beneath northwest part of South America during Late Cretaceous.

In this work, an oceanic plateau is described as a large area (at least 10^5 km²), formed many million years ago due to the decompressing melting of mid-ocean ridges, characterized by olivine cumulates in the lowermost layers and overlain by isotropic gabbros. The base of the oceanic plateau is composed of geochemically heterogeneous high-MgO lavas that are, in turn, succeeded upward by relatively homogeneous basaltic lavas. Moreover, the oceanic plateaus, in general, have a thickness of at least 2-3 km around the surrounding sea floor by which its areas are difficult to subduct, and their uppermost sections are accreted to continental margins (Kerr et. al., 2014; Kerr, 2015)

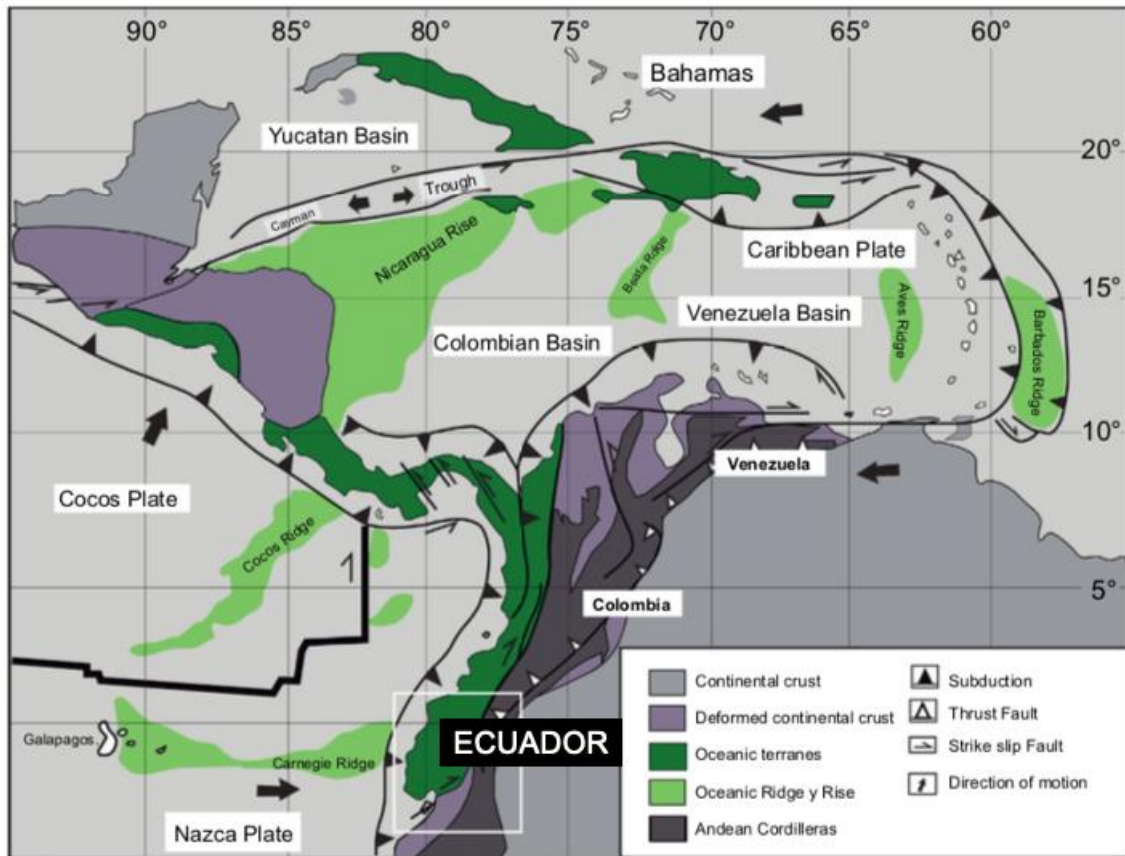


Figure 1. Regional map showing the plate tectonic framework of the Northern Andes and the Caribbean region taken from (Vallejo et al., 2019). The white square, in the south part, displays the location of Ecuador, where the study area is included.

The Caribbean oceanic plateau is of Turonian-Coniacian (Fig. 2) (≈ 90 Ma) age, which is documented by Kerr et al. (2005) with radiogenic isotope studies of komatiites, picrites, and basalts taken in Gorgona Island, Colombia. The birth of Caribbean oceanic plateau was in the Pacific Ocean, where a hot spot was erupted through the Farallón plate, of which the oceanic plateau was a part of. Moreover, the onset of subduction-related magmatism in the Middle Campanian (≈ 80 Ma) suggests that from then on, the COP was separated from the Farallón Plate by a subduction zone, and constituted an individualized tectonic plate. (Jaillard et al., 2007; Kerr et al., 2005). Thus, the creation of this northeast subduction zone related as part of the northern edge collision of Caribbean oceanic plateau against Central American continental blocks, and the significant clockwise rotation of Farallón plate, Jaillard et al. (2007), interpreted the San Juan Terrain, which is a unit of Ecuador that outcrop along a narrow belt in the western part of the Interandean valley, and at the eastern border of the Western Cordillera, as accretion in Late Campanian (≈ 75 Ma).

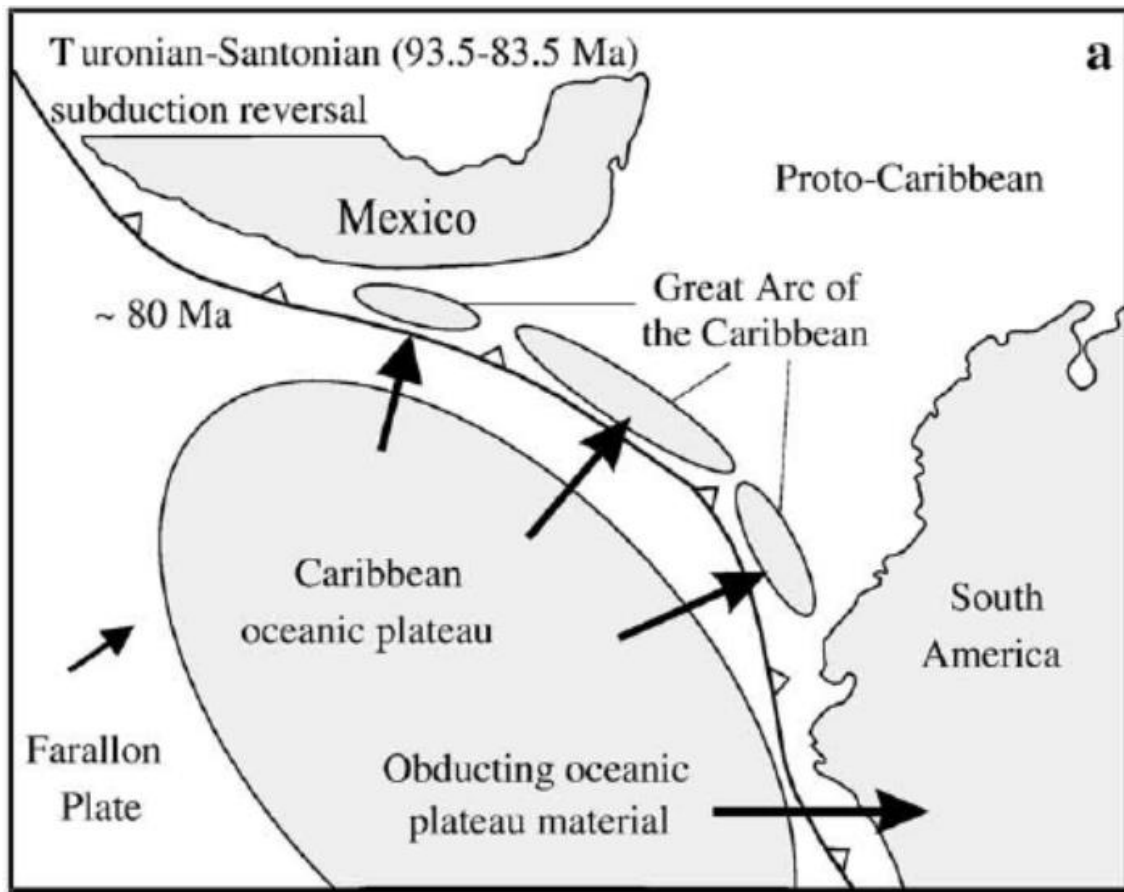


Figure 2. Schematic representation of birth of the Caribbean oceanic plateau when belonged to the Farallon plate and collide with South America plate (Kerr et al., 1999).

On the other hand, the fragments of the new oceanic plate formed by the separation of the Farallón plate, collide in Late Maastrichtian to the Ecuadorian Margin which produce a reorganization of the subduction zones, development of a new arc system, resulting in the accretion of a volcanic terrain called the Guaranda Terrain (Jaillard et al., 2007; Kerr et al., 2005). Moreover, Jaillard et al. (2007) interpret the Piñon terrain accreted in the Late Paleocene to the Ecuadorian margin as new fragments of Caribbean oceanic Plateau, which has been divided into several fragments throughout its history. This evolution of Caribbean oceanic plateau and Ecuadorian margin have created a forearc system through all the Ecuadorian coast.

In Ecuador, an effort to understand the subduction, accretion and collision of the Caribbean Plateau with the South American Plate have been carried out. For example, geochemical analysis of the basement rocks of the Ecuadorian forearc have demonstrated an equivalent with fragments of the Caribbean Plateau that formed around 87 to 100 Ma (Kerr et al., 2005; Vallejo et al., 2019). In addition, Jaillard et al. (2007) have shown that

the western part of Ecuador is composed by several oceanic terranes accreted to the Andean margin during the Late Campanian to Late Paleocene periods.

1.2. Rationale

Tectono-sedimentary works in the northern Ecuadorian margin proposing an evolution of the depositional environments controlled by tectonic processes are missing in the literature. In Delgado and Lucas (2018), a tectono-stratigraphy analysis of Esmeraldas-Borbón basin is described. However, sedimentary features, such as lithological information from wells and outcrops or detailed geometries in seismic-stratigraphic sequences, are still lacking. Consequently, a 4D tectonic evolution is waiting to be developed.

Describing the tectonic-sedimentary evolution of a part of the Ecuadorian margin from the Cretaceous to Neogene is relevant to understand better the evolution of the accretion of the oceanic terrains. Likewise, it can contribute for future works on hydrocarbon explorations. It is well known the existence of hydrocarbon fields in the southern coastal part of Ecuador (Jaillard et al., 1995) and there may be more in the northern coastal part.

1.3. The Esmeraldas-Borbón Basin

The Cretaceous to Neogene sedimentary succession of the northwestern part of the Ecuadorian margin (Fig. 3) provides an opportunity to study the tectono-sedimentary evolution related to the Caribbean and South American plate interactions. The Esmeraldas-Borbón Basin is located in this region, which is part of the Ecuadorian forearc (Deniaud et al., 1999; Jaillard et al., 2007). This basin has been poorly studied due to lack of access to this place because it is mostly covered by dense vegetation. However, the existence of Cretaceous to Neogene successions has been described (Reyes and Michaud, 2012; Lopez, 2007; Marcaillou, 2008). Moreover, unpublished seismic reflection surveys have been obtained in this area.



Figure 3. Geological sketch map showing the main tectonic provinces of Ecuador. Thus, this map indicates the principal basin and fault systems that control the geology of Ecuador (modified from maps Deniaud et al., 1999; Vallejo et al., 2019; Luzieux, 2006). Black square indicates location of Figure 5.

1.4. Objectives

In this study, I use unpublished seismic reflection and well data set from the Esmeraldas-Borbón Basin in conjunction with field observation to: (i) characterize the tectonic structure of a part of this basin; and (ii) establish relations between tectonic structures and stratigraphic thickness and lithological distributions through the time. The aim of my work is to produce a tectono-sedimentary evolution of a part of the Esmeraldas-Borbón Basin. This work should contribute to the knowledge of the interaction history between the Caribbean and South American plates.

CHAPTER 2: GEOLOGICAL SETTING

2.1. Geological features of a forearc region

Forearc basins are regions in a subduction zone between the outer-arc high and the volcanic arc (Fig. 4). These types of basins develop as a result of an oceanic plate subducting beneath other plates, which can be oceanic or continental plate (Lutz et al., 2011). The forearc basins, due to this location, provide information about subduction zone dynamics, which are interacting process between the subducting oceanic plate and the overriding forearc crust (Noda, 2016). Moreover, these basins are important in relationship to understand earthquakes, sediment transport and deposition, and the accumulation of petroleum and gas hydrocarbons (Lutz et al., 2011; Wells et al., 2003; Matsumoto et al., 2011).

Volcanic Arc System

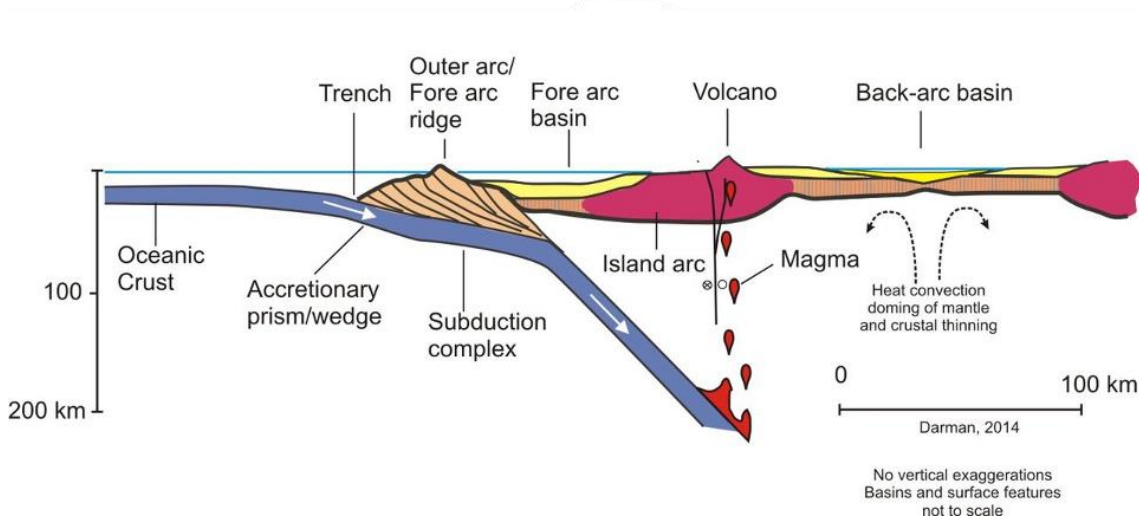


Figure 4. Schematic cross-section of a volcanic arc system (Darman, 2014). In the left part of the section, a fore arc basin is shown in yellow color, formed due to subduction of oceanic crust (blue color).

2.2. Regional features

The principal basins in the Ecuadorian forearc region, from south to north, are: Gulf of Guayaquil; El Progreso; Manabí and Esmeraldas-Borbón basins (Fig. 5). In south Colombia, the forearc area is characterized by two main basins: the Manglares Basin, which extend also to north Ecuador; and the Tumaco Basin.

From a regional point of view, the Esmeraldas-Borbón Basin extends to the Colombian border (northeast; Fig.5), where the basin is limited by the so-called Mataje Fault (López-Ramos, 2009). To the southeast, this basin is limited by the Western Cordillera. To the southwest, it is bounded by a WSW-ENE striking Quinindé Fault, and to the northwest, the basin is delimited by a structural high referred as Rio Verde high (Reyes and Michaud, 2012; Collot et al., 2019; Delgado and Lucas, 2018).

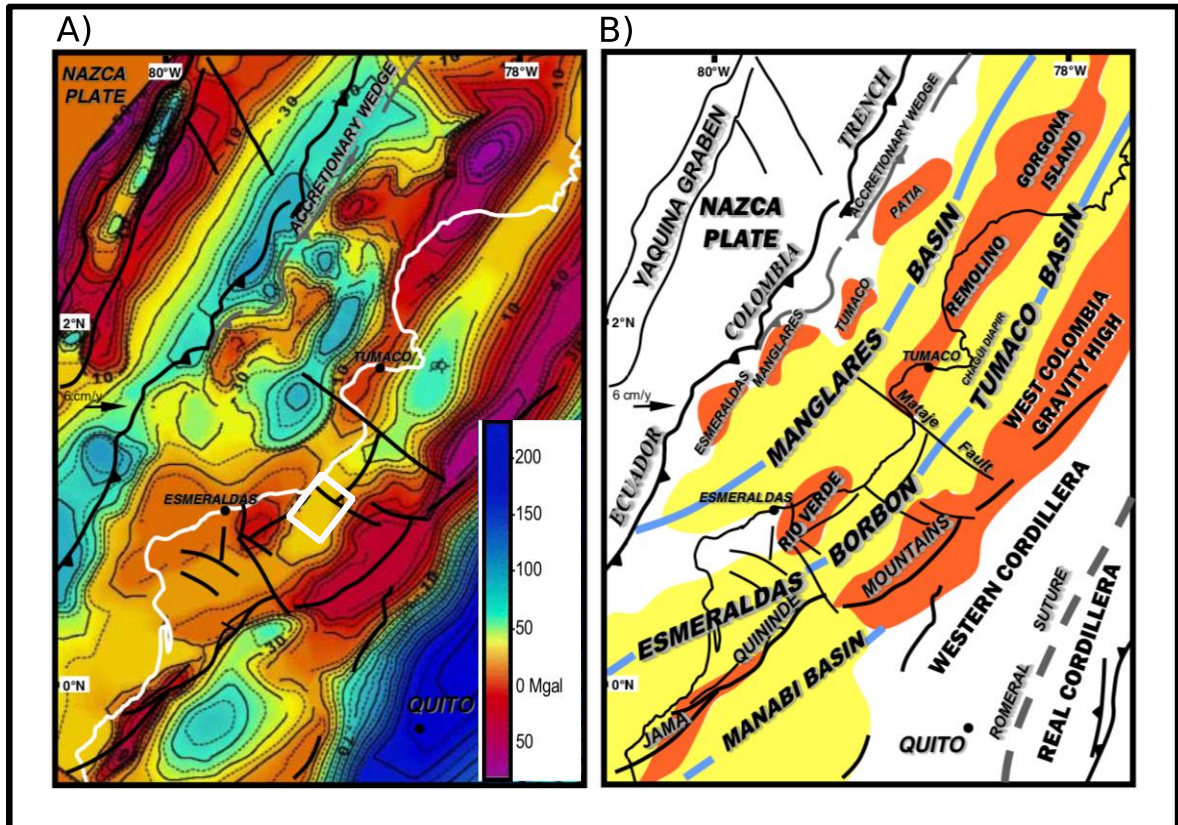


Figure 5. a) Gravimetric map showing the boundaries of the Southern Colombia and Northern Ecuador forearc basins. Study area is represented (white frame); b) Distribution of basins (in yellow), axis of basin (in blue) and structural highs (in orange) (Lopez, 2007).

2.3. Stratigraphy

In previous works (Luzieux, 2006; Vallejo et al., 2019; Reyes and Michaud, 2012), it is recognized that the Ecuadorian forearc is composed by a regional Cretaceous basement and a Paleocene to Quaternary sedimentary cover. For the purpose of this study, the following nine lithostratigraphic units are considered, from older to younger: 1) Piñón (Late Cretaceous); 2) Cayo (Late Santonian-Maastrichtian); 3) Zapallo (Middle to Late Eocene); 4) Playa Rica (Early Oligocene) 5) Pambil (Early to Late Oligocene); 6) Viche (Early to Middle Miocene); 7) Angostura (Late Miocene) ; 8) Ónzole (Late Miocene and

Pliocene); and 9) Cachabí (Pliocene to Early Pleistocene) formations (Fig. 6). The basement is composed by the Piñón and Cayo formations. The mineralogy, lithology, depositional environment and age of all these units are described as follows.

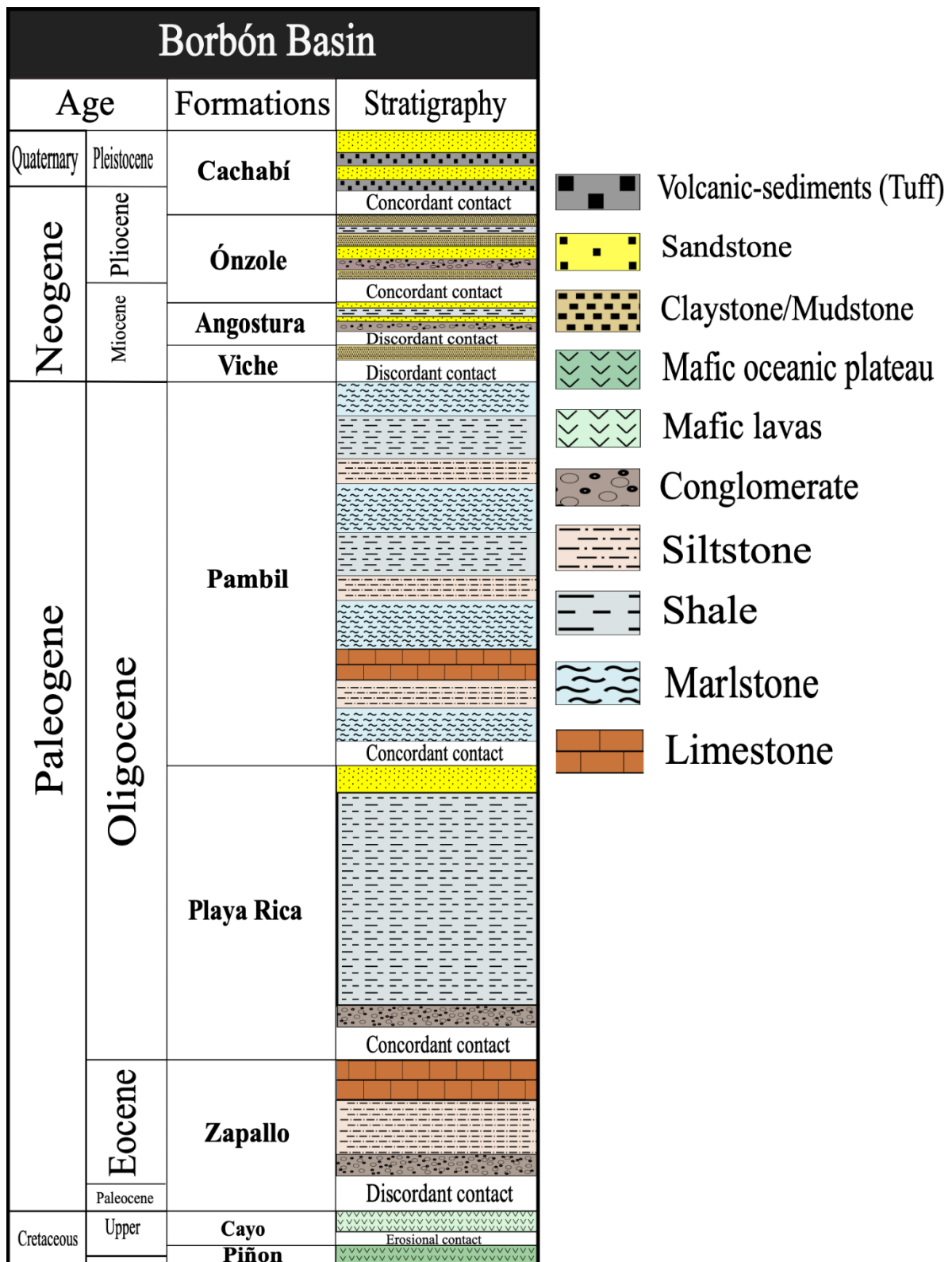


Figure 6. Stratigraphic column of Esmeraldas-Borbón Basin. This graph represents the chronostratigraphic and lithological information of the study area. This column was made with information from a review of the literature and well data (Reyes and Michaud, 2012; Vallejo et al., 2019; Delgado and Lucas; 2018; Ordoñez et al., 2006; Luzieux et al., 2006).

2.2.1. Piñon Formation (KPñ)

The Piñon formation (KPñ) (Fig. 7A) is considered as the regional basement of the entire coastal forearc due to its appearance in some parts such as the Chongon - Colonche Cordillera to the northern part of the Gulf of Guayaquil and the Manabí Basin (Vallejo et al., 2019).

The Piñon formation is principally composed by an extensive range of volcanic rocks with mafic composition. The lithologies include an igneous complex formed by extrusive rocks characterized by pillow basalts, aphanitic basalts interbedded with breccias. In smaller portion of tuff argillites, siltstone and sandstone (Ordoñez et al., 2006). Furthermore, in studies documented by Luzieux et al., (2006), the pillow geometries contain clinopyroxene and plagioclase phenocryst enclosed in a groundmass constituted of quenched plagioclase, and clinopyroxene microlites. Likewise, there are picritic hyaloclastites composed of glass which are replaced by palagonite having picritic and basaltic fragments.

In the southern part of the Ecuadorian coast, the Piñón Fm is overlain by the Cayo Fm (Bristow & Hoffstetter, 1977), which is eroded towards the north (Evans & Arguello, 1977).

The formation has an age older than 98.4 Ma, which belongs to the Cretaceous. It has been inferred by Macias (2018) based on U-Pb analysis obtained from zircons in cross-cutting intrusions. However, Vallejo et al. (2019) have obtained an age ranging between 98.4 ± 1.7 Ma and 90 ± 1.6 Ma, which belong to Cenomanian-Turonian age.

2.2.2. Cayo Formation (KCy)

The Cayo Formation (KCy) (Fig. 7A) is mainly composed by volcano-derived debris-flow, and silicified turbidites (Luzieux et al., 2006; Vallejo et al., 2019; Reyes and Michaud, 2012). Furthermore, in the upper part, there is a finer grained accompanied by a gradual increase in the fraction of bioclasts that are dominant at the top. These bioclasts are composed by sponge spicules and radiolarian skeletons which are mainly responsible for siliceous cementation in this upper part of the formation (Luzieux et al., 2006).

The turbiditic and debris flow facies are interpreted to be the result of lateral migration of mid- and lower submarine fan setting (Luzieux et al., 2006; Vallejo et al., 2019). The flow of these facies observed in the San Lorenzo block indicate NE to SW direction (Luzieux et al., 2006).

Radiolaria, foraminifera and dinocysts association in the upper strata of the formation indicates a depositional age corresponding to the Late Santonian-Maastrichtian age (Luzieux et al., 2006).

2.2.3. Zapallo Formation (EZp)

In this formation (EZp) (Fig. 7A) there is a clastic succession with medium to fine grains (Reyes and Michaud, 2012). Furthermore, the Zapallo Formation is constituted by white and greyish shales, siliceous claystones and siltstones with intercalated thin layers of tuffs, sandstones and sandy limestones. These lithologies overlie discordantly (unconformity) a basal conglomerate composed by clasts of basalt and limestone with a grain-size of pebble (Luzieux et al., 2006).

The depositional environment of this formation is inferred as neritic in a mixed siliciclastic-carbonate platform (Luzieux et al., 2006).

Due to rich benthonic fauna and abundant foraminiferal remains, the Zapallo Formation is considered as a Middle to Late Eocene deposit (Luzieux et al., 2006; Kerr et al., 2002).

2.2.4. Playa Rica Formation (OPr)

This formation (OPr) (Fig. 7A) para-conformably overlies the Zapallo Formation. Likewise, Playa Rica Formation is composed by monotonous succession of dark grey siltstones and shales (Luzieux et al., 2006).

According to Canfield (1966), the depositional environment of the Playa Rica Formation corresponds to a deep marine to shallow deposition facies.

The age of this formation based on previous works from Olsson (1942), and Canfield (1966) on the basis of radiolarian assemblages shows that this formation was deposited during the Early Oligocene (Luzieux et al., 2006).

2.2.5. Pambil Formation (OPm)

Pambil Formation (OPm) (Fig. 7A) is a massive sedimentary succession of blue-gray pelitic rocks (Reyes and Michaud, 2012). Likewise, there is a monotonous green-gray massive shale, marlstone and siltstone with beds of sandstones and tuffs (Luzieux et al., 2006; Vallejo et al., 2019). This formation concordantly overlays the Playa Rica Formation (Bristow & Hoffstetter, 1977).

Radiolarian associations are found at the base of the Pambil Formation and benthic foraminifera in its upper part (Whittaker, 1998; Luzieux et al., 2006). This fact allows to infer a shallowing-upward trend in a deep marine to shallow environments.

The formation is considered as Early to Late Oligocene based on the microfossil association (Luzieux et al., 2006).

2.2.6. Viche Formation (MVh-Db)

The Viche Formation (MVh-Db) (Fig. 7A) is composed by silty and clay successions with calcareous lenses. Furthermore, this formation consists of green-gray and brown mudstones, tuff shales with green-gray or blue-gray colors (Jiménez et al., 2007, Luzieux et al., 2006). This Formation discordantly overlies the Pambil Formation (Bristow & Hoffstetter, 1977).

In the formation there are nannofossils, foraminifera, radiolarians and palynomorphs that represent deposits of marine environment from external platform to upper slope. The observed change recognized by Luzieux et al. (2006) of facies from the Viche to the Angostura Formation was most likely driven by a westward progradation of the coastal system.

These microfossil association testify the Early to Middle Miocene age (Jiménez et al., 2007).

2.2.7. Angostura Formation (MAG)

The Angostura Formation (MAG) (Fig. 7A) is composed by a basal conglomerate interval. Overlying this interval, there is a massive sandstone and siltstone succession. Sandstones are yellow to red in color, coarse grained with a few feldspars and abundant quartz abundance, locally presenting cross-bedding. Moreover, the sandstones and siltstones become finer westward where inter-bedded mudstones are dominant (Jiménez et al.,

2007; Díaz, 2013). These lithology discordantly overlies the Viche Formation (Bristow & Hoffstetter, 1977).

The lithologies together with the microfossil association occurring in this formation determine a marine paleoenvironment characterized by a deep platform.

The microfossil association prove a Late Miocene age of deposition (Jiménez et al., 2007).

2.2.8. Ónzole Formation (MOz)

This formation (MOz) (Fig. 7A) is divided into two members: the lower part and upper part. These members are separated by the Sua sandstone Member (Delgado and Lucas, 2018). The lower Onzole member is constituted by well-stratified sandstone and siltstone. It is dark green-gray in color. The Sua Member is composed by conglomerate, and sandstones of medium- to fine grain, it is yellow to orange in color, and it has a good stratification. On the other hand, the upper Onzole member is composed by fine grain pelitic layers with turbiditic facies and bioturbation occurs. Furthermore, there is volcanic ash and glauconite deposits. The Onzole Formation concordantly overlies the Angostura Formation.

The Lower Onzole member is interpreted to be deposited in an outer platform environment. The paleoenvironment of the upper Onzole member is interpreted as paleoenvironment of platform external to continental slope (Díaz, 2013).

According to Luzieux et al. (2006), the deposition ages of Ónzole formation belong to the Late Miocene and Pliocene.

2.2.9. Cachabi Formation (PLB-Ch)

The Cachabi Formation (PLB-Ch) (Fig. 7A) or also called Borbón Formation is composed by volcanic and clastic lithologies. The clastic part is composed by fine- to medium- grained sandstones, grey and yellow-brown in color, and is interbedded by the volcanic part that is composed by tuff, and clays with greenish gray tuff sandstone interbedded (Ramirez, 2013; Reyes and Michaud, 2012). This formation concordantly overlies the Onzole Formation (Reyes and Michaud, 2012).

Sediments, mainly claystone and interbedded fine-grained sandstone, indicate a shallow to outer shelf paleoenvironment (Ordoñez et al., 2006).

The estimated depositional age of the Cachabi Formation is Pliocene to Early Pleistocene (Díaz, 2013; Marcaillou, 2008; Reyes and Michaud, 2012).

2.3. Structural Features

In the surface of the Esmeraldas-Borbón Basin there are two principal WSW-ENE-striking faults, the Canande Fault (F10 in Fig. 7A) and Tanigüe Fault (F11 in Fig. 7A). Furthermore, in this basin, a dome and two main SW-NE trending folds are present.

The Canandé Fault, which is a N-dipping reverse fault (Fig. 7B), controls the outcrops of the basement. The Tanigüe Fault is a N-dipping normal fault (Fig. 7B).

The core of the domes is formed of the basement. The two folds consist of an anticlinal, located in the center part of the Esmeraldas-Borbón Basin, and a syncline, to the east of this basin (Reyes and Michaud, 2012).

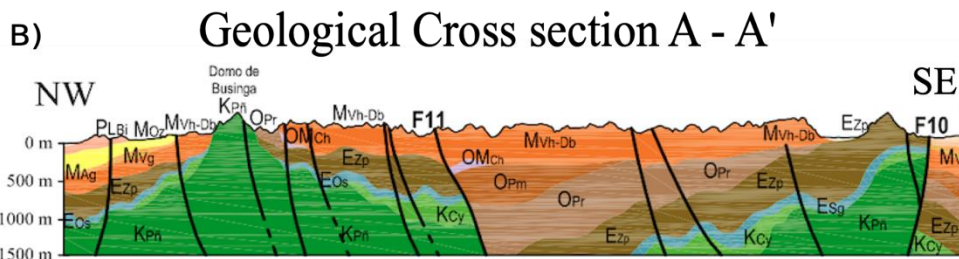
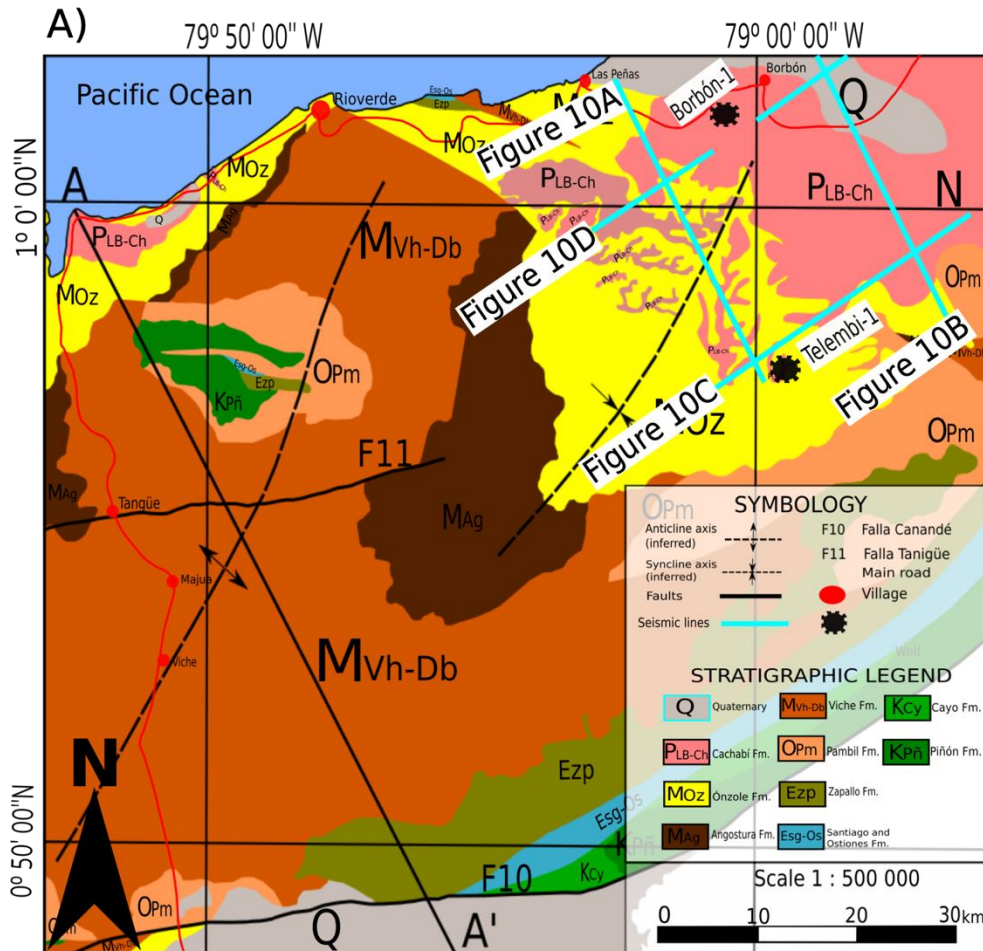


Figure 7. a) Northern part of Esmeraldas-Borbón Basin where is presented the principal formation, structures (faults and folds), and the seismic lines used in this work as well as a cross-section. The study area of this work is represented by the seismic lines (light blue). b) Cross Section (A-A') (Reyes and Michaud, 2012).

CHAPTER 3: DATA SET AND METHODS

3.1. Data set

This study uses eight two-dimensional (2-D) seismic reflection profiles located in the study area (Fig. 7A) and oriented NW-SE (perpendicular to the main structural trend) and SW-NE (parallel to the main structural trend). These seismic profiles were provided by *Secretaria de Hidrocarburos del Ecuador* (SHE). The seismic lines are presented in two-way travel-time (TWTT). Based on a depth vs. time plot (Fig. 8), derived from checkshot data from wells in the Manglares and Tumaco basins and documented in López (2007), an estimated average velocity of the sedimentary cover of ca. 3050 m/s is considered in the present work. Structural and stratigraphic features observed are herein described using seconds and meters using this velocity. Subsurface data is provided by logs of the Borbón-1 and Telembi-1 wells. In both wells, there are information about short normal and long normal resistivity and the spontaneous potential that has a unit of millivolts.

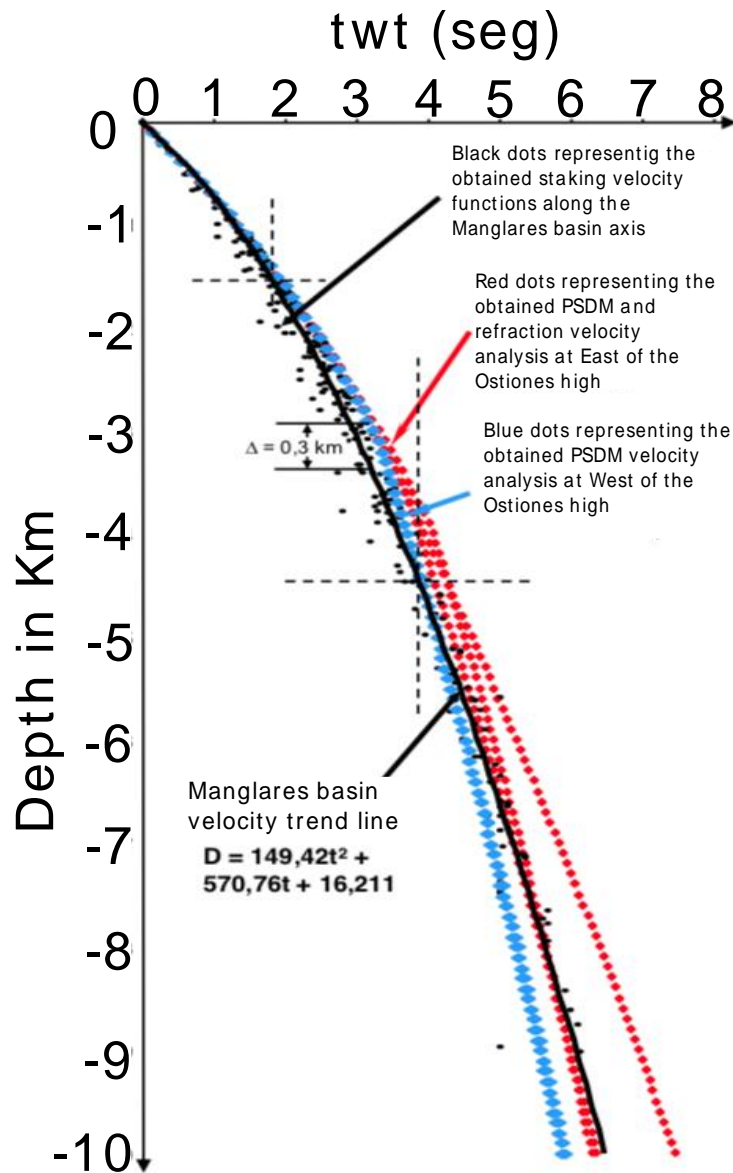


Figure 8. Depth vs time plot calculated from 25 stacking velocity functions along the Manglares Basin, and the curve is based on Pre-Stack Depth Migration (PSDM) velocity analysis and seismic refraction along the same basin depocenters axis (Lopez, 2007; Collot et al., 2008).

3.2. Methodology

3.2.1. Depositional sequences and sedimentary framework

All the seismic lines were referred to a same reference datum (0 s equal to 15 m above mean sea level) and tied to the wells (Fig. 10 and 12). In these lines, for understanding the structures controlling the sedimentation, relevant structural features and depositional sequences were identified and mapped (Fig. 11). The depositional sequences were characterized using reflector properties, such as amplitude, continuity, frequency, which was determined visually, and comparing the number of traces for giving amount of time

and configuration of seismic reflections. A pattern of this characterization is shown in Figure 9.

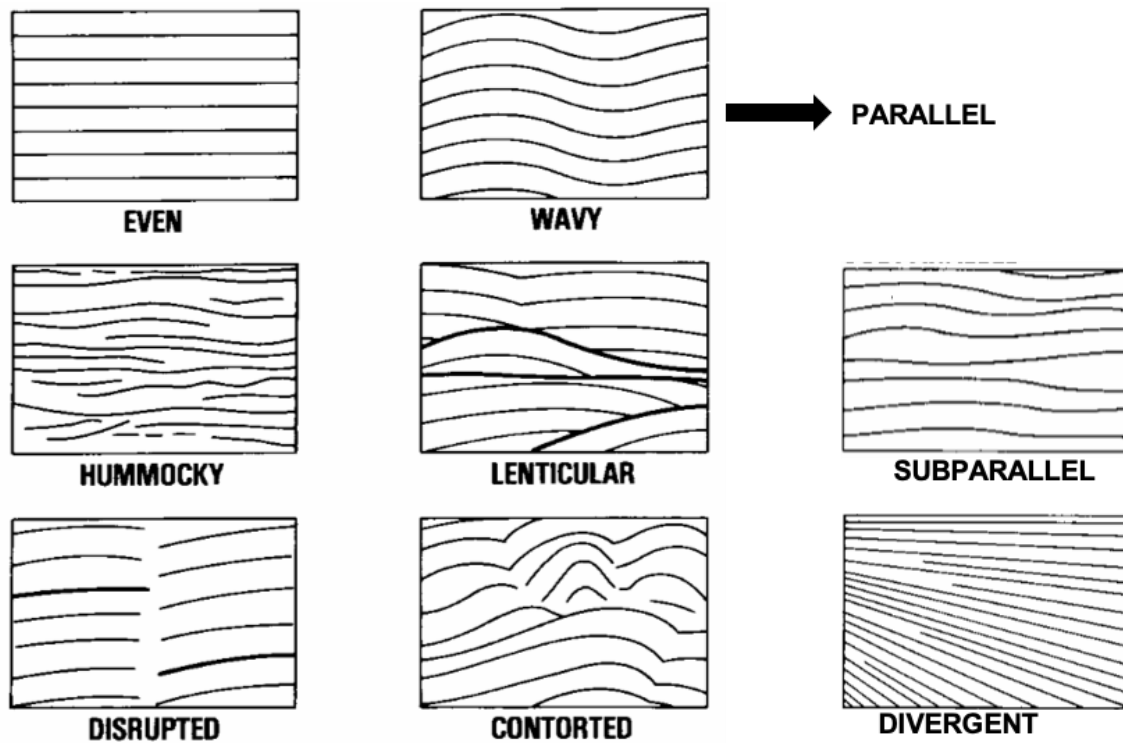


Figure 9. Schematic illustration of some seismic reflection configuration (Mitchum et al., 1977). The seismic facies configuration classification are used to interpret the facies type from the seismic reflector information.

In order to know the composition of the depositional sequences, a lithological characterization from wells (Fig. 12) was carried out. Thus, it generated eight lithostratigraphic sections (sections A to H in Fig. 10). The lithostratigraphic sections were completed with information obtained from previous work. To highlight lateral sedimentation distributions, a stratigraphic correlation was generated by incorporating these data. Also, isopach maps of relevant sequences were made up (Fig. 13).

3.2.2. Interpretation and regional framework

For the interpretation of the tectono-sedimentary evolution in the study area, three paleogeographic maps, known as Stage 1, Stage 2 and Stage 3 (Fig 16A, B and C), were produced. These maps were based on the lithology of the Borbón-1 and Telemi-1 wells (Fig. 12), the structural features (Figs. 10 and 11) and the isopach maps (Fig. 13).

CHAPTER 4: RESULTS

In this work, I observed the existence of at least nine depositional sequences in the study area (Fig. 10A). From older to younger, these sequences are referred to herein as A, B, C, D, E, F, G, and H. The seismic-stratigraphic character and geographical distribution, involved structures, thickness distribution and lithology variations of each sequence are described in the following sections.

4.1. A Sequence

This sequence is composed by two seismic facies. The first seismic facies, referred to herein as “A1”, has high amplitude, medium continuity, medium to high frequency and the configuration of the seismic reflections is disrupted (Fig. 10A). This seismic facies is located in the upper-most part of the sequence. The second seismic facies, referred to here as “A2”, which is below A1, has low amplitude, low continuity, the frequency is medium to low, and the configuration of seismic reflection is chaotic. The seismic facies A1 prevails in the northernmost part of the study area. By contrast, the seismic facies A2 prevails in the southernmost part of this area. Moreover, the geometry in the upper part of A1 presents a top-lap to the B Sequence while in the lower part the signal is lost as depth increases.

The sequence A is affected by three principal faults, referred herein as F1, F2, and F3 with a N-S strike (Figs. 10A and B). The first fault (F1) is located in the southwestern part of study area having a reverse geometry and a throw at the top of the sequence of 130 ms (ca. 200 m). In this fault is observed that there is more thickness in the hanging wall than in the footwall of A Sequence. The second fault (F2) is situated in the southeastern part of study area (Fig. 7A), with a reverse displacement and a throw at the top of the sequence of 800 ms (ca. 1220 m). The third fault (F3) is located in the northeastern part of the study area having a reverse geometry and a throw at the top of the sequence of 130 ms (ca. 200m). Moreover, small faults, called here F4, F5 and F6, with a small throws (<100 ms) at the top of the sequence are also present. Furthermore, the faults F3 and F6 has less thickness in the hanging wall of A Sequence. This sequence is also deformed by a main anticline, called A1 (Fig 10C) and located in the south part of study area (Fig. 7A), with an SW-NE orientation and a curvature of $0,0008 \text{ m}^{-1}$.

The main lithologies of the A Sequence are recognized in the wells (Fig. 12). In the depth interval of 1400 to 1800 m of the Telembi-1 well, porphyritic lava and volcanic material were encountered.

4.2. B Sequence

The B Sequence is characterized by B1, which has attributes of high amplitude, medium continuity, high frequency and the configuration of seismic reflectors are sub-parallel (Fig. 10 A). The reflectors with high amplitude are observed from north to south onlapping the A Sequence.

This sequence is affected by the F2 fault which has a reverse geometry and N-S strike. This sequence is also affected by the F3, F4, F5 and F6 faults, and is observed that the faults F4 and F5 erode this formation Likewise, the B Sequence is affected by the A2 anticline (Fig. 10C), and located in the south part of study area (Fig. 7A), with an SW-NE orientation and a curvature of $0,0007 \text{ m}^{-1}$.

In the Borbon-1 well, this sequence has a thickness of 200 m in the interval depths of 2900 to 3100 m. In the Telembi-1 well, the thickness of the B Sequence is 200 m in the interval depths of 1200 to 1400 m (Fig 12). In the study area, the maximum thickness of the B and C Sequences reaches up to 700 ms (ca. 1068 m; Fig. 13.A) where presently, a structural depression in the top of the A Sequence exists. In the present day the anticline A1 (Fig. 10C), a 300 ms (ca. 458 m) structural relieve is recognized.

The main lithologies of the B Sequence are recognized in the wells (Fig. 12). In the depth interval of 1400 to 1200 m corresponding to the Telembi-1 well, limestones and shales are encountered. In the depth intervals of 3100 to 2900 m of the Borbón-1 well, shale and siltstone are observed.

4.3. C Sequence

The C Sequence is composed by one seismic facies (C1), which has medium amplitude, the continuity is medium to high, the frequency is medium, and the seismic reflection configuration is divergent (Fig. 10A). In this sequence there are more reflectors with high amplitude in the southern part. The boundary in the upper part is concordant with sequence D while the boundary in the lower part is onlapping on sequence B.

This sequence is affected by the fault F2 which has a reverse geometry and N-S strike (Figs. 10 B), and is deformed by the fault F6. This sequence is also affected by an

anticline, A3 (Fig 10A), located in the eastern part of the study area (Fig. 7A), with a NW-SE orientation and a curvature of $0,0007 \text{ m}^{-1}$. Likewise, this fold is observed in the Figure 10B, with an axis that has an orientation NE-SW.

In the Borbon-1 well, a thickness of 400 m in the interval depths of 2900 to 2500 m is identified. In the Telembi-1 well, the thickness of the B Sequence is 400 m in the interval depths of 1200 to 800 m (Fig 12). In the study area, the structural relieve distribution of this sequence is the same that the described in the B sequence (Fig. 13A).

The main lithologies of the C Sequence are recognized in the wells (Fig. 12). In the depth interval of 1200 to 800 m of the Telembi-1 well, shales, calcareous shales, calcareous sand, sand, and conglomerates are identified. In the depth intervals of 2900 to 2500 m of the Borbón-1 well, shale with small beds of siltstone, siltstone, sandstone and tuffaceous shale are recognized. At the top of this succession, conglomerates are identified.

4.4. D Sequence

The D Sequence is composed by one seismic facies, D1, which has high amplitude, medium to high continuity, high frequency, and the configuration of seismic reflection is parallel disrupted (Fig. 10 A). The seismic facies D1 is located in the southern part. The boundaries of this sequence are erosional with the C Sequence below and the E Sequence above.

This sequence is affected by the faults F2 and F3. In the fault F2 the D sequence shows a change in thickness, which produce a more thickness on the footwall than in the hanging wall of this sequence. The F3 fault has a reverse geometry and N-S strike. Likewise, this sequence undergoes a change on thickness due to the anticline A3 (Figs. 10B). The D Sequence has a well-marked subsidence of 300 ms (ca. 458 m; Fig. 10C). This subsidence is located in the south part of the study area (Fig. 7A).

The D Sequence has in the Borbon-1 well a thickness of 200 m in the interval depths of 2500 to 2300 m. In the Telembi-1 well the thickness of D Sequence is 500 m in the interval depths of 800 to 300 m (Fig 12). In the study area, the maximum thickness of the C and D Sequences reaches up to 600 ms (ca. 915 m; Fig. 13B) where, at present day, a structural depression in the top of the D Sequence exists. In the present day, the structural high relieve has 300 ms (ca. 458 m).

The main lithologies of the D Sequence are recognized in the wells (Fig. 12). In the depth interval of 800 to 300 m corresponding the Telembi-1 well, shales, calcareous shales, and

sandstone are observed. In the depth intervals of 2500 to 2300 m corresponding to the Borbón-1 well, there are siltstone and shale in the base, and in the upper part with a small thickness there are beds of calcareous sand and limestone.

4.5. E Sequence

This sequence is composed by one seismic facies (E1), which has low amplitude, medium to low continuity, the frequency is medium to low, and the configuration of seismic reflection is subparallel disrupted. The reflectors with high amplitude are shown from the north to south of this sequence. Furthermore, the boundaries of the sequence E in the lower part is onlap, and the upper boundary there is a concordance contact (Fig. 10A).

The E Sequence is affected by the fault F3 which has a reverse geometry and N-S strike (Figs. 10 B).

In the Borbon-1 well, this sequence has a thickness of 1000 m in the interval depths of 2300 to 1300 m (Fig. 12). In the Telembi-1 well the E Sequence does not appear. In the study area, the maximum thickness of the D, E and F Sequences reaches up to 1000 ms (ca. 1525 m; Fig. 13C) where, at present day, a structural depression in the top of the E Sequence exists. In the present day structural highs reach up a 500 ms (ca. 763 m) of structural relieve.

The main lithologies of the E Sequence are identified in the well (Fig. 12). In the depth interval of 2300 to 1300 m corresponding to the Borbón-1 well, which there are an interbedded between conglomerates, sandstone, and calcareous shale in the base. Afterwards, in the middle of this sequence, there is a calcareous sand with thin beds of limestone. In the top of the sequence there are beds of siltstone, sandstone, and calcareous shale.

4.6. F Sequence

The sequence F is constituted by three seismic facies. The first seismic facies, called F1 has low amplitude, low continuity, frequency medium to low, and the configuration of seismic reflection is chaotic. This seismic facies is located in the lower part of this sequence. The second facies recognized in this sequence is called F2 that has a high amplitude, high continuity, high frequency, and seismic reflection configuration is parallel. The boundaries of this sequence are concordant with the E Sequence below and the G Sequence above (Fig 10A).

This sequence presents a pinch-out in the southern part of study area (Fig. 10B) due to slip of the F2 fault.

In the Borbon-1 well, this sequence has a thickness of 300 m in the interval depths of 1300 to 1000 m (Fig. 12). In the Telembi-1 well the thickness of sequence F is 100 m in the interval depths of 300 to 200 m. In the study area, the thickness distribution of this sequence is the same described for the E sequence (Fig. 13C).

The main lithologies of the F Sequence are documented in the wells (Fig. 12). In the depth interval of 300 to 200 m corresponds to Telembi-1 well, calcareous shales, sandstone, and limestones are encountered. The depth intervals of 1300 to 1000 m corresponds to the Borbón-1 well, where there are tuffaceous shale, interbedded of calcareous silt, and sandstone with some thin layers of limestones.

4.7. G Sequence

This sequence is composed by a seismic facies G1, which has high amplitude, medium to high continuity, medium frequency, and seismic reflection configuration is parallel. The reflectors with highest amplitude and frequency are located in the northernmost part of this sequence (Fig. 10A). The boundary in the lower part is concordant with F Sequence, and the boundary in the upper part is toplap with H Sequence.

The sequence G has in the Borbon-1 well, a thickness of 400 m in the interval depths of 1000 to 600 m (Fig 12). In the Telembi-1 well there is no G Sequence.

The main lithologies of the G Sequence are recognized in Borbón-1 well. In the base of this sequence there is a calcareous shale with some thin layers of siltstone and sandstone. Furthermore, there is a layer of sandstone until an interbedded of calcareous shale, siltstone, and shale with thin layers of sandstone.

4.8. H Sequence

The sequence H is composed by seismic facies H1 that has medium amplitude, medium to low continuity, the frequency is medium to low, and the configuration of the seismic reflection is chaotic. The reflectors, in this sequence, has a medium amplitude from north to south (Fig. 10A). The boundaries of this sequence are onlap with G Sequence in the lower part, and erosional surface in the upper part.

The H Sequence has in the Borbon-1 well a thickness of 400 m in the interval depths of 600 to 200 m (Fig 12). In the Telembi-1 well there is no H sequence.

The main lithologies of the G Sequence are identified in the Borbón-1 well. In the base of this sequence there is a calcareous shale with some thin layers of siltstone and sandstone. Furthermore, there is a layer of sandstone until an interbedded of calcareous shale, siltstone, and shale with thin layers of sandstone.

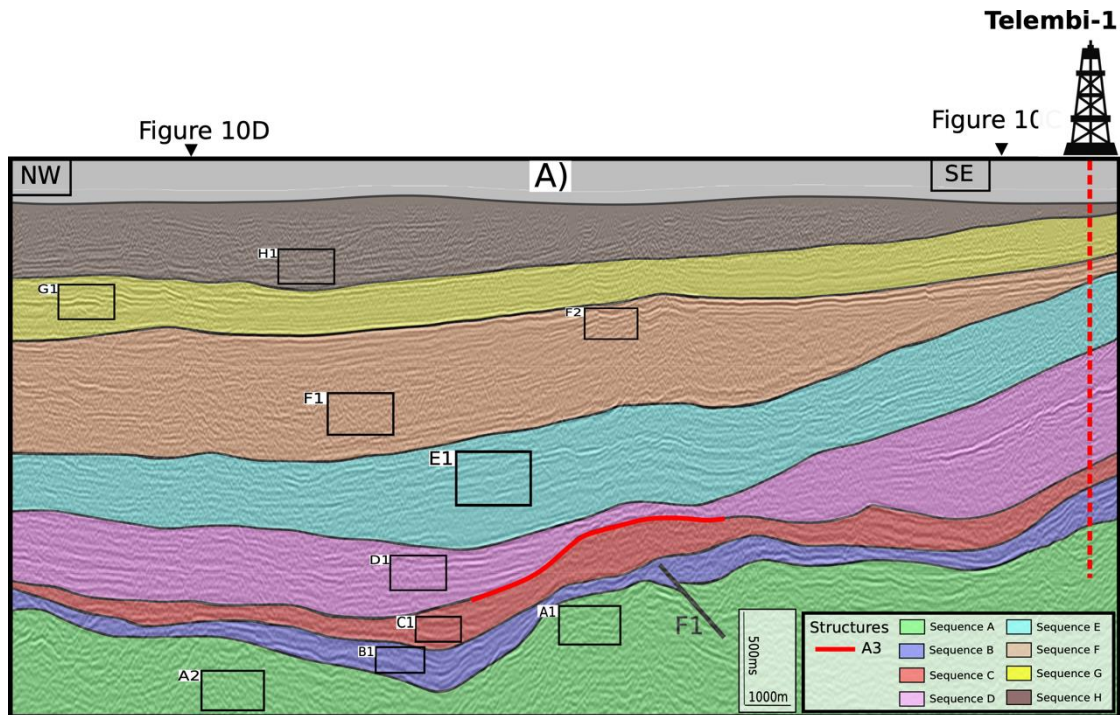


Figure 10. Seismic lines of key sections in the study area (Fig.7A). Triangles situated at top of the lines, indicate the intersection with other sections. A3 represent the anticline structures described in the results of each sequence. The well-marked subsidence of sequence D is represented in the line C, and the truncated reflectors are represented with arrows. The seismic lines are presented in two-way travel-time (TWTT).

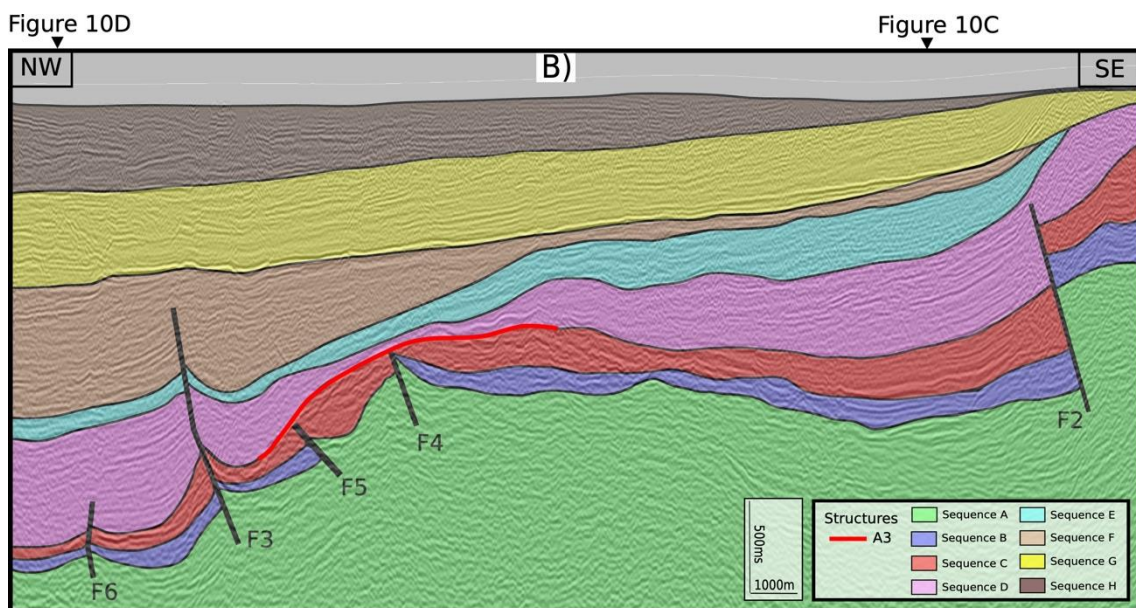


Figure 10 Continued.

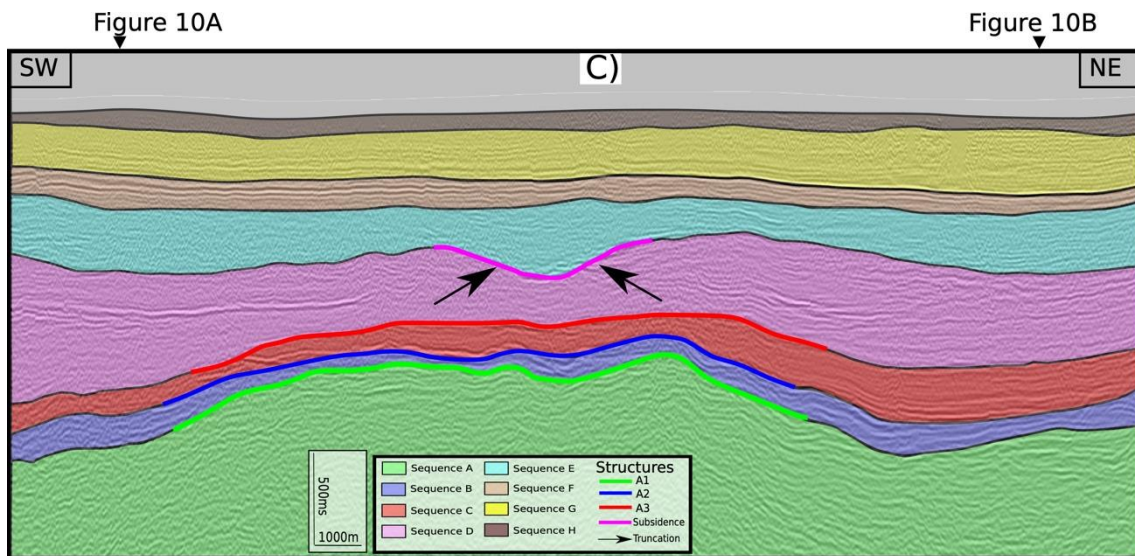


Figure 10 Continued.

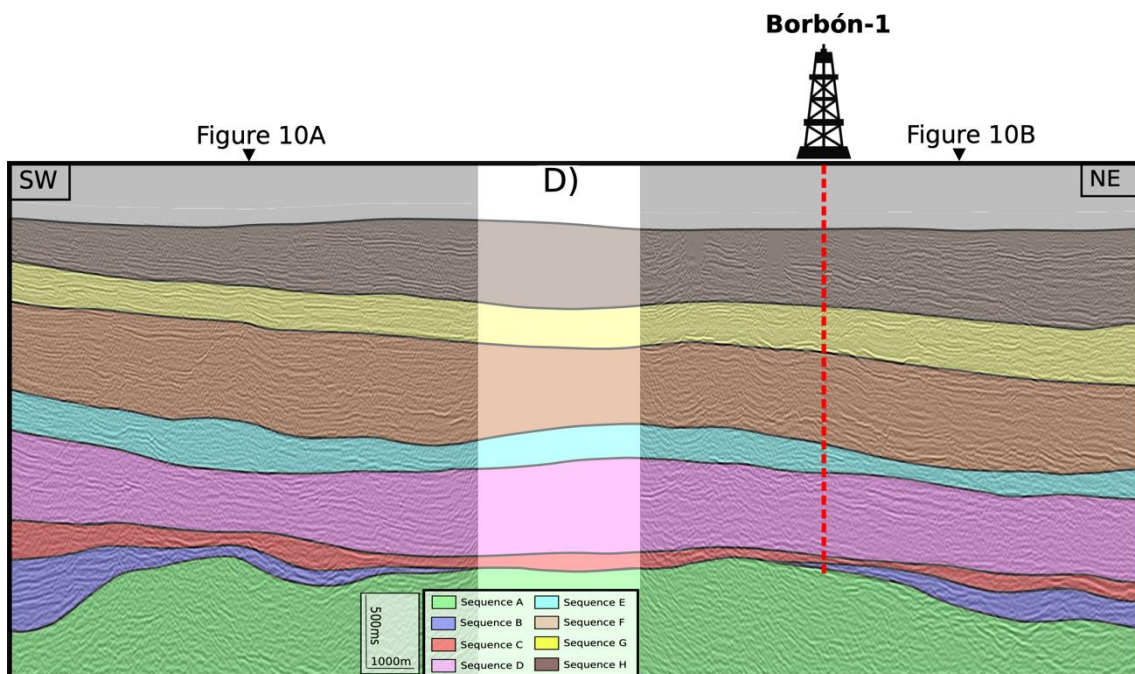


Figure 10 Continued.

A)

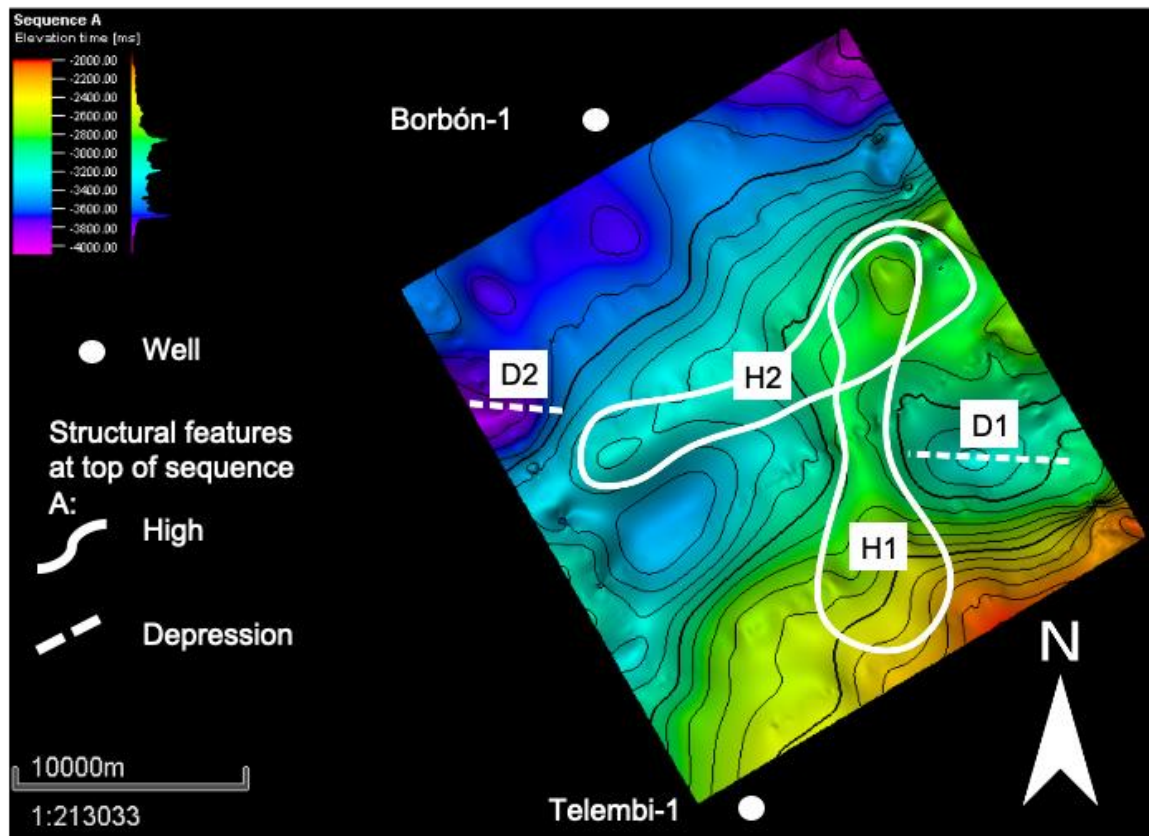


Figure 11. Structural maps of the study area. A) Top of Sequence A; B) Top of Sequence C; C) Top of Sequence D. The number represents the label of each structural highs and depressions.

B)

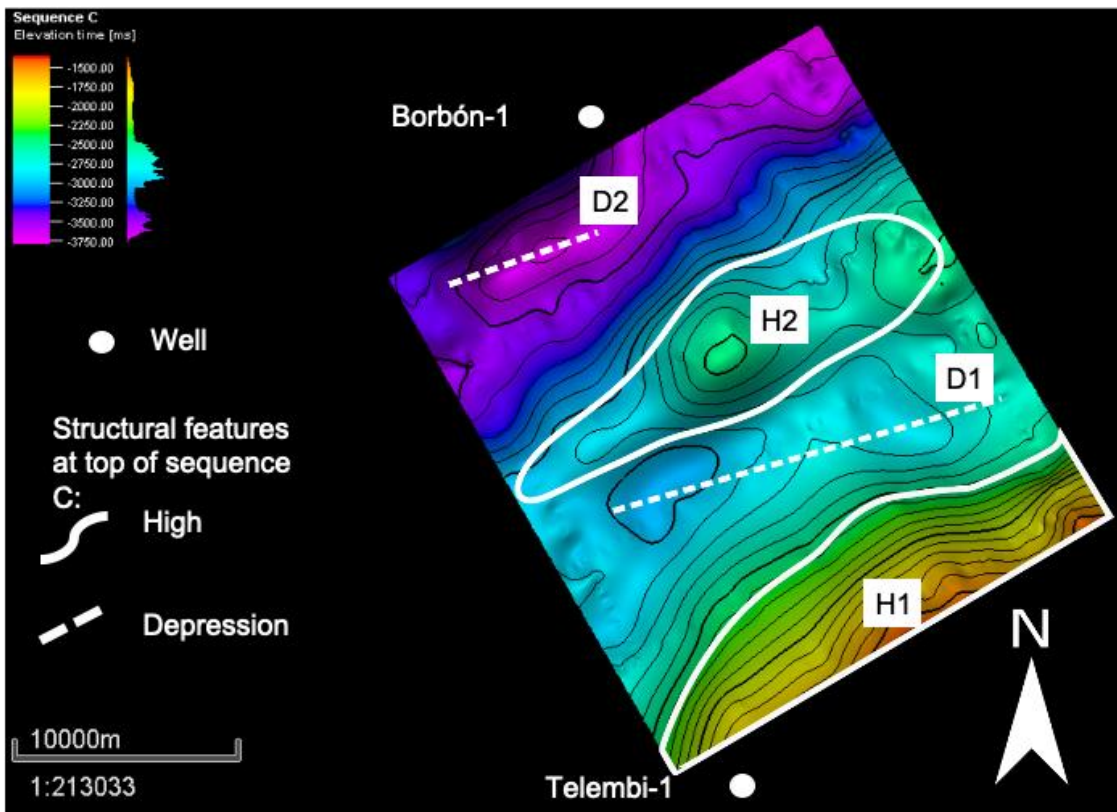


Figure 11. Continued.

C)

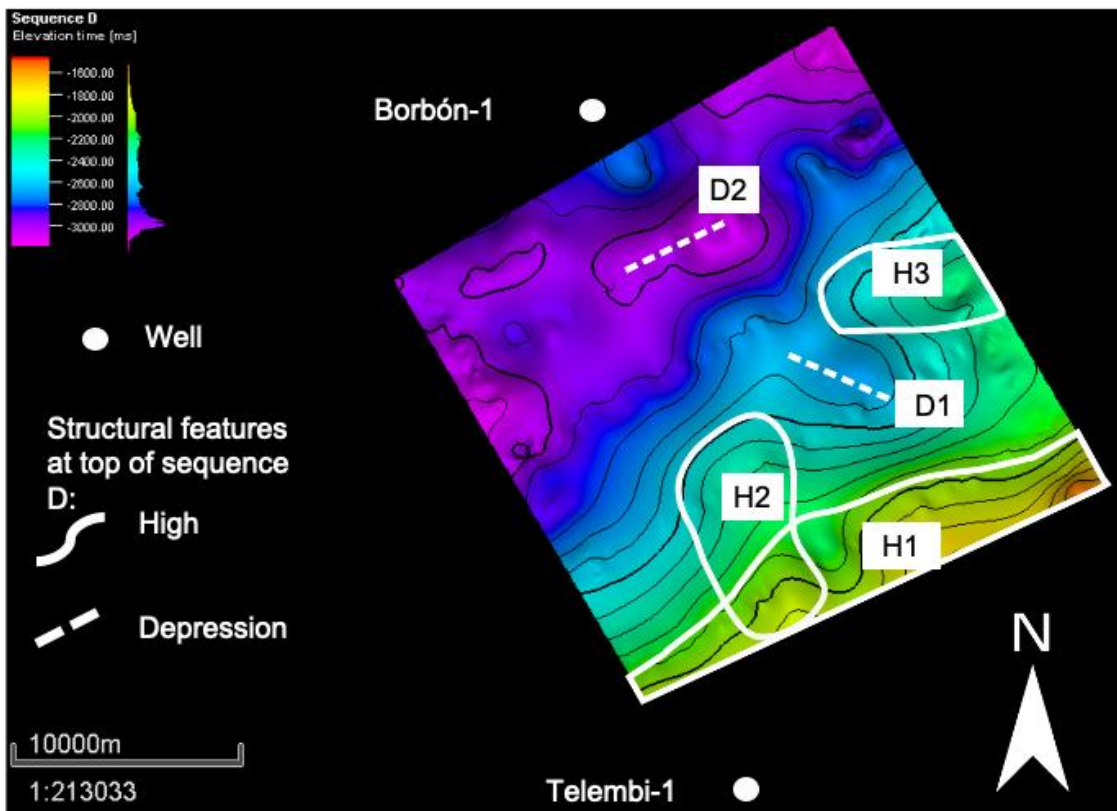


Figure 11. Continued.

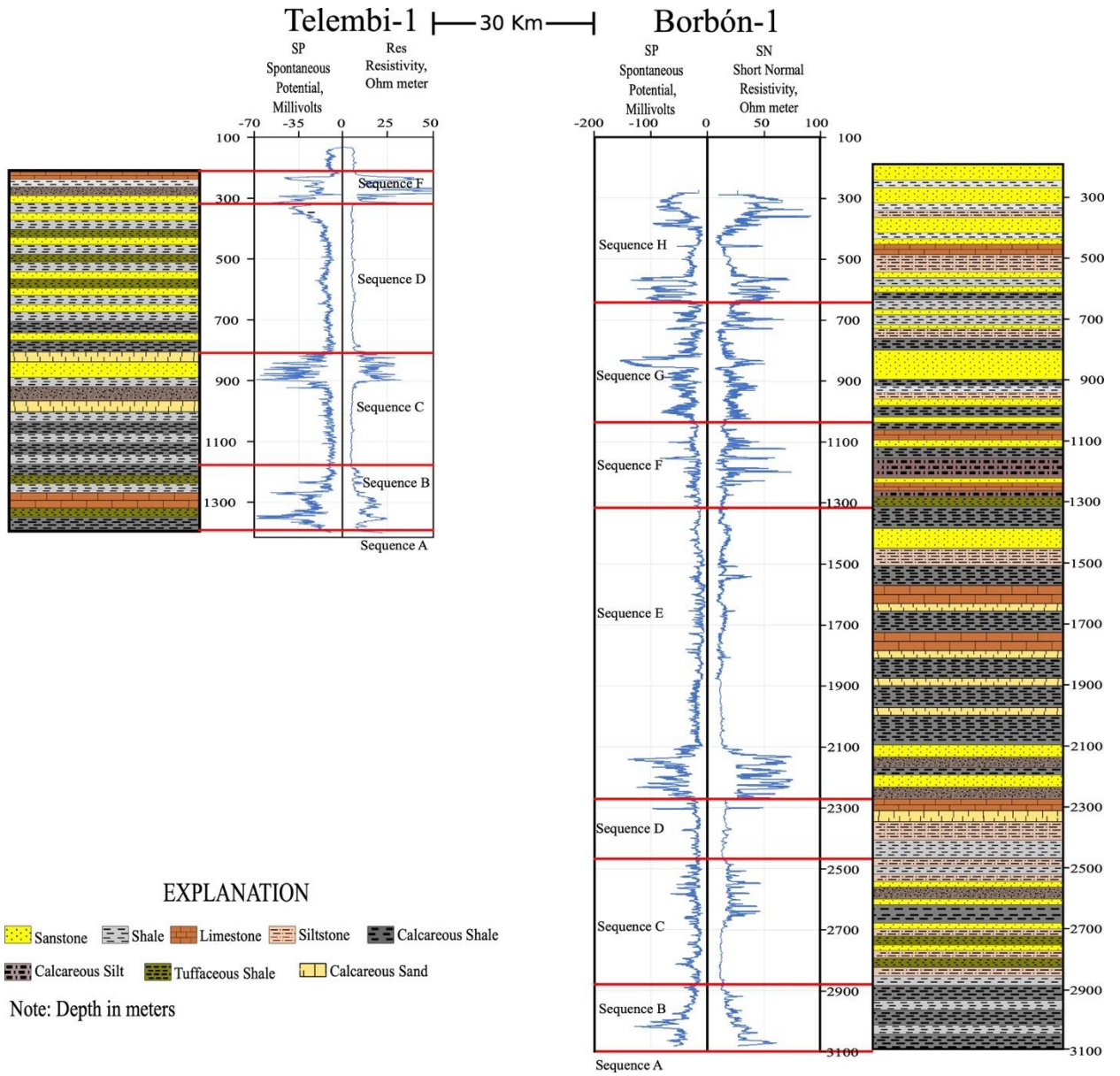


Figure 12. Correlation between Telembi-1 and Borbón-1 well. The wellsshow lithologies and short normal and long normal resistivity, and the spontaneous potential logs that have units of millivolts (X axis), and meters (Y-axis).

A)

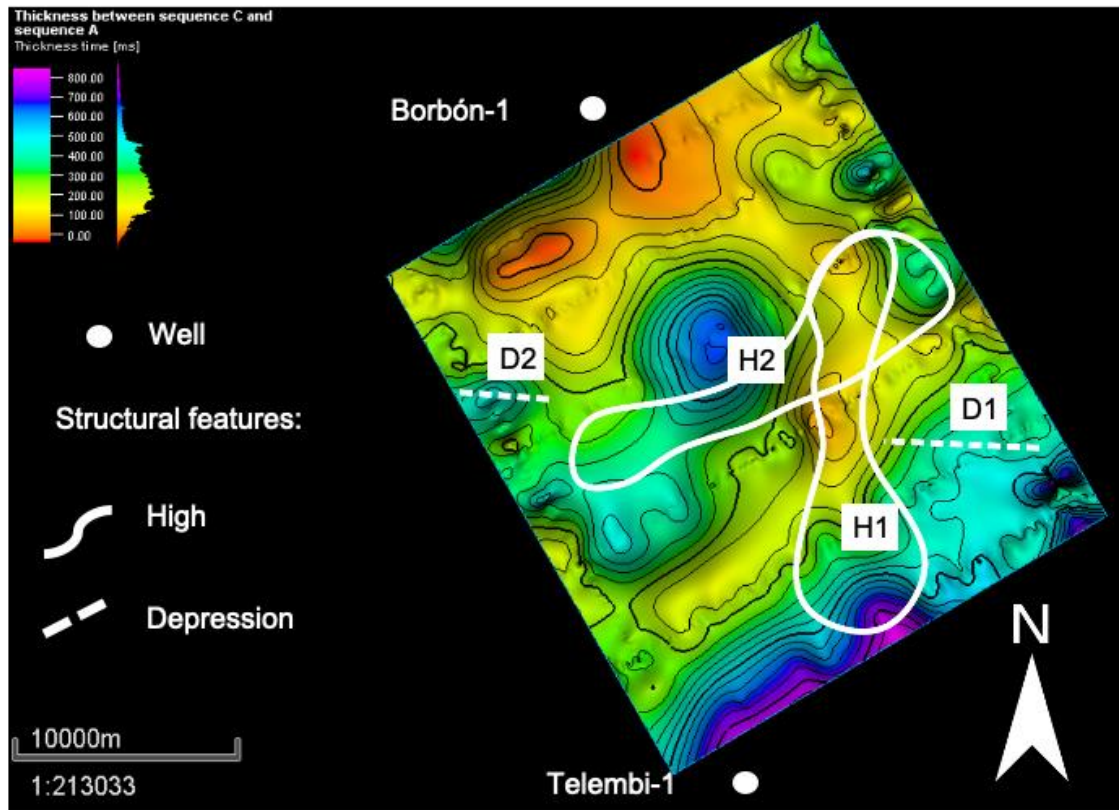


Figure 13. Isopach maps. A) Thickness between the sequences A and C; B) Thickness between the Sequences C and D; C) Thickness between the Sequences D and F. The numbers represent structural highs and depressions defined in Fig 11.

B)

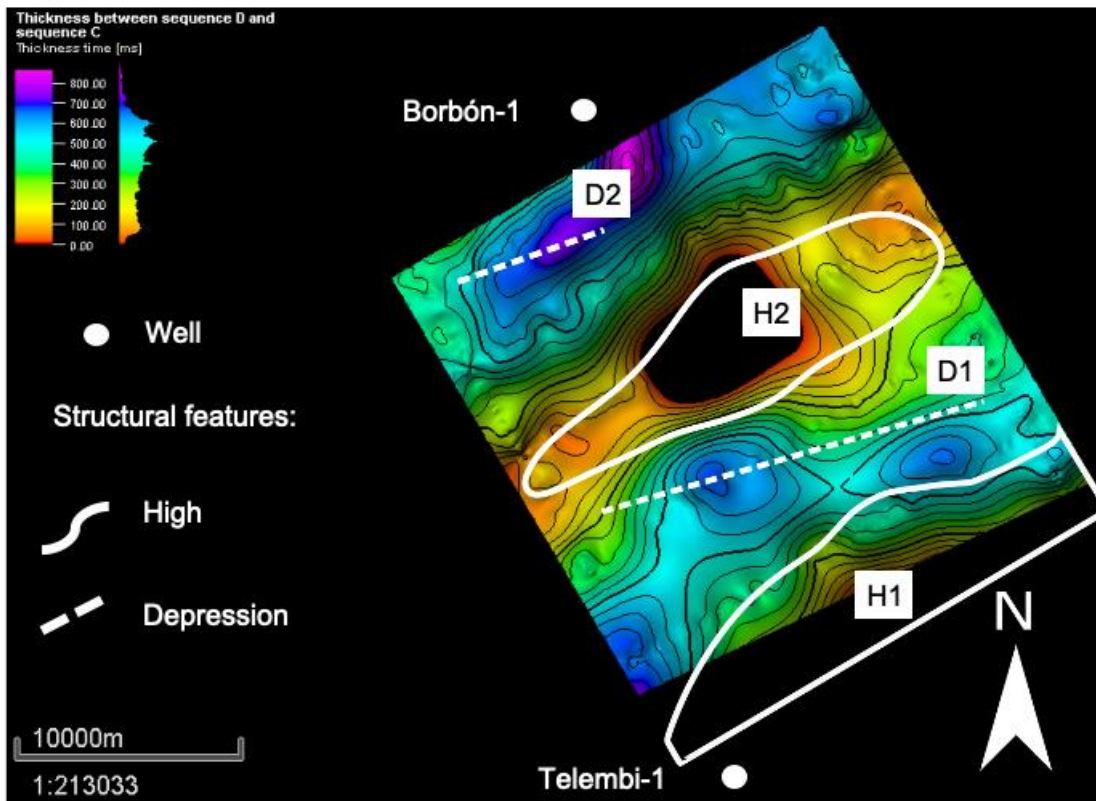


Figure 13. Continued.

C)

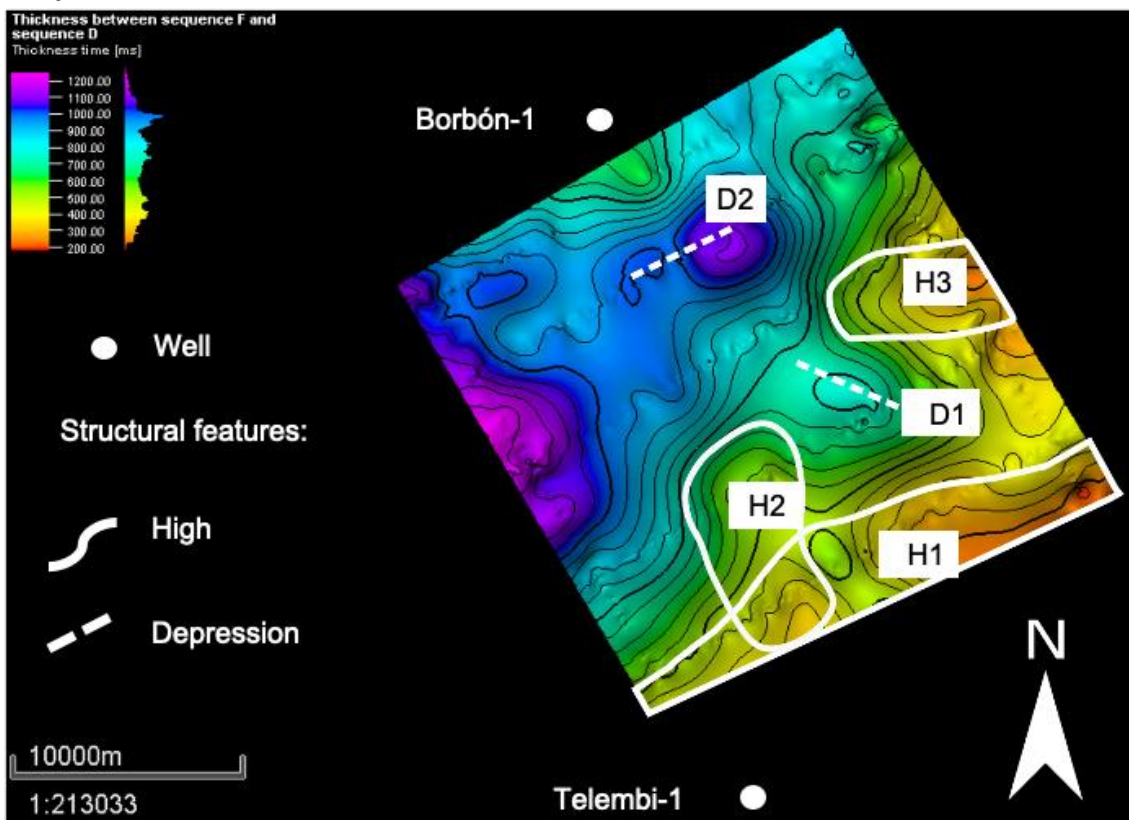


Figure 13. Continued.

CHAPTER 5: DISCUSSION

5.1. Chronostratigraphic Relationship

In this work, based on the observations of the lithologies made on the Borbón-1 and Telembi-1 wells (Fig. 12), the depositional sequences were correlated with the formations documented in the Esmeraldas-Borbón Basin (Fig. 6). This correlation is shown in Table 1 and in the Figure 14.

Table 1. Lithology correlation between sequences and formations.

Agea	Sequence	Lithology	Formation
Late Cretaceous	A	Lavas; mafic material	Piñon
Eocene	B	Limestones	Zapallo
Early Oligocene	C	Shales	Playa Rica
Late Oligocene	D	Shales; siltstones	Pambil
Early Miocene	E	Shale; siltstone; limestone	Viche
Late Miocene	F	Conglomerates; sandstones	Angostura
Pliocene	G	Sandstones; calcareous shales	Ónzole
Pleistocene	H	Sandstones; siltstones; shales	Cachabí

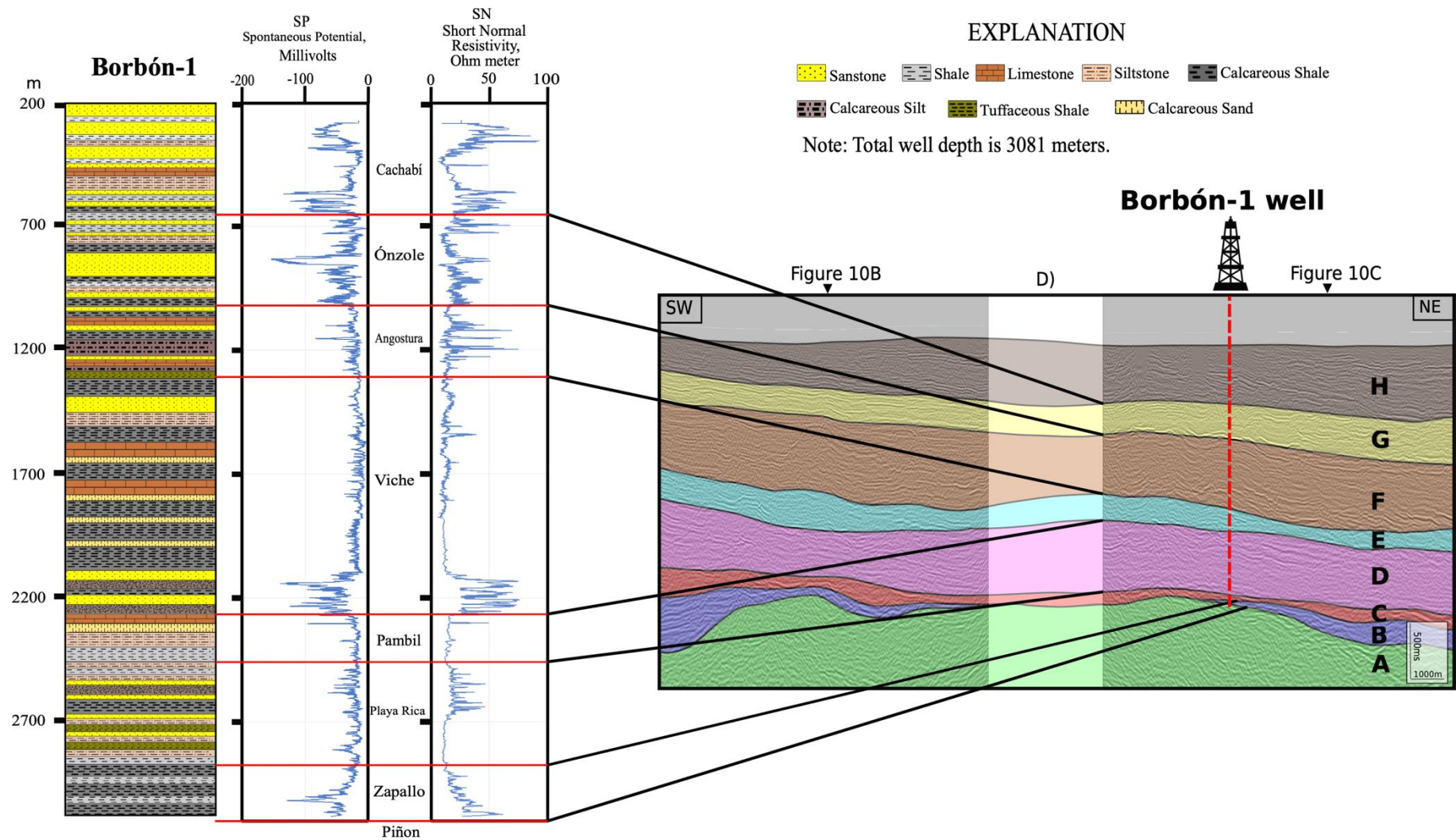


Figure 14. Correlation between Borbón-1 well and seismic line (Fig. 10D). This graph shown the sequences found in the area of study and the location of the well Borbón-1. The triangles show the intersecting profiles (Fig. 7A).

5.2 Structural Interpretation

In the sequence D (Pambil Formation) the change in thickness due to the anticlinal A3 (Fig. 10A and B). This anticlinal A3 undergoes an uplifting caused by fault in the Piñon Formation, which is missed in basement because of poor continuity of reflectors.

The difference on thickness caused by fault F2 (Fig 10B) on Pambil Formation makes that this Formation has a change in thickness. Therefore, in Pambil Formation there are more thickness on the footwall of the fault F2 because of it is syn-tectonic event. On the other hand, the thickening of Zapallo formation in the hanging-wall of fault F1 is interpreted as a normal fault during the deposition of the Piñon and Zapallo Formations, and then an inversion that caused the reverse fault F1 (Fig. 10B). Moreover, the faults F4 and F5 (Fig. 10B) are cutting the Piñon Formation and erode the Zapallo Formation. This mean that the faults F4 and F5 are younger than the deposition of Zapallo Formation. The fault F6 (Fig. 10B) is cutting since Piñon to Pambil Formations, and the thinning in the hanging wall of this fault is interpreted as a syn-tectonic event. Likewise, the fault F3 (Fig. 10B) are cutting since the basement to Angostura Formation. This fault is interpreted as syn-tectonic due to there is more thickness on the footwall of fault F3. Therefore, all of these faults ended while Ónzole and Cachabi Formations were depositing. Thus, the faults F3, F4, F5, and F6 are older than the Ónzole and Cachabi Formations.

The configuration of structural highs a structural depressions present a change through stage 1, stage 2, and stage 3 (Fig. 15). The changes are in relief because the position of structural highs and depression are maintained in the same position thought all stages. Thus, this configuration produces a 2 structural high belt and between them two structural depression belt. Therefore, I interpret the structural configuration of my study area as two shifting due to the faults F1, F2, F3, F4, F5 and F6. This produce a piggy-back basins on the structural depressions. However, based on the work of Michaud (2015), the north of Esmeraldas-Borbón Basin is controlled by dipping faults, which tend to coalesce downward forming a flower structure. Therefore, the structural interpretation is open to discussion.

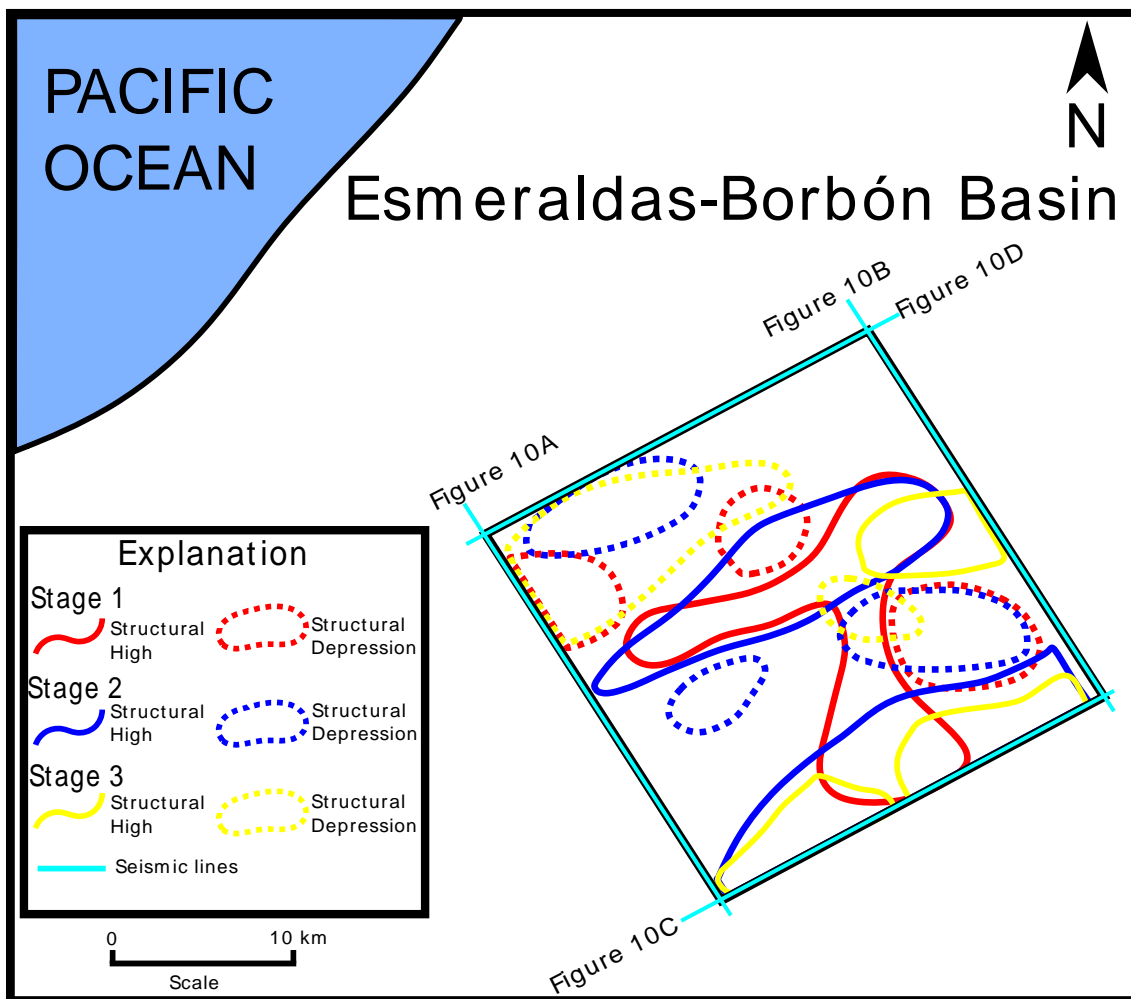


Figure 15. Structural map evolution of the study area shown the movement of the structural highs and structural depression through stage 1 (Late Cretaceous to Early Oligocene), stage 2 (Early to Late Oligocene), and stage 3 (Late Oligocene to Late Miocene). Based on the isopach maps (Fig. 11), the structural depressions correspond to the outline 800 ms, and the structural highs correspond to the outline -200 ms.

5.3. Tectono-sedimentary evolution

I propose three paleogeographic maps that correspond to the tectono-sedimentary evolution between the Late Cretaceous and Late Oligocene in the study area. These maps, referred herein as Stage 1, Stage 2 and Stage 3, include the evolution of the structures described in Chapter 4 and correspond to the following sedimentary stages and formations: Stage 1 (Fig. 16A), Late Cretaceous to Early Oligocene, Zapallo and Playa Rica formations; Stage 2 (Fig. 16B), Early to Late Oligocene, Pambil formations; and Stage 3 (Fig. 16C), Late Oligocene to Late Miocene, Viche Formation and Angostura formations.

5.3.1. Stage 1: Late Cretaceous to Early Oligocene

Stratigraphic thinning of the Zapallo and Playa Rica formations toward the structural highs (H1 and H2) and the northward depression (D2) (Figs. 11A and 13A) suggests that these highs and depression were uplifting during Stage 1 (Fig. 16A). Likewise, in the southeast part of the map there is a thickening, which means that during the Eocene there were structural depressions.

Based on the relationships between thickness distribution of the B and C Sequences (Fig. 13A), and the lithology of the Borbon-1 and Telembi-1 wells (Fig. 12), the following tectono-sedimentary features are interpreted for Stage 1: in agreement with López (2007), and Marcaillou (2008), limestones are deposited in the structural highs, and shales in structural depressions (Fig. 16A). Thus, the limestones belong to shallow platform, and shales corresponds to deep platform.

5.3.2. Stage 2: Early to Late Oligocene

The stratigraphic thinning of the Pambil Formation toward the structural high (H2 and H1) in the central and southern part of the map (Figs. 11B and 13B) suggest that there was a tectonic uplift with direction SW-NE, which is seen in the seismic lines (Fig. 10A and 10B). Furthermore, according to the observations made on Fig. 13B there is a thickening toward structural depression (D1 and D2). This suggest that during Early to Late Oligocene there were structural depression.

Based on the lithological distribution of the Borbón-1 and Telembi-1 wells (Fig. 12) and the thickness distribution of the Pambil Formation (Fig. 13B), the following tectono-sedimentary features are described for this stage: sandstones in the structural highs; and mudstones in the structural depressions, and there are limestones in the most distal part of study area (Fig. 16B). Therefore, in agreement to López (2007) the sandstones correspond to shallow platform and mudstones belong to deep platform.

5.3.3. Stage 3: Late Oligocene to Late Miocene

Stratigraphic thinning of the Pambil and Viche formations toward the structural highs (H1, H2 and H3), and the northward depression (Figs. 11C and 13C) suggest that these highs and depression were uplifting during the Stage 1. Furthermore, based on the

observation of Fig. 13 C there is a thickening in toward depression (D1, and D2). This suggest that during Oligocene-Miocene there were structural eastern depression. In addition, the marked erosive surface of the D Sequence and its geometry (Fig. 10 C) suggests the existence of paleo-valleys from the structural highs to the structural depressions.

Based on the relationships between thickness distribution of the VicheB and Angostura Formations (Figs 13C), which is controlled by the structural highs, and lithology of Borbón-1 and Telemi-1 (Fig- 12), the following tectono-sedimentary features are interpreted for Stage 1: In agreement with López (2007), sandstones in eastern depression and paleo-valleys; and mudstones with sandstones on the structural highs (Fig. 16C). Hence, the sandstones in the eastern depression and paleo-valleys corresponds to submarine fan-lobes and turbiditic channels, respectively. The mudstones and sandstones are attributed to shallow platform.

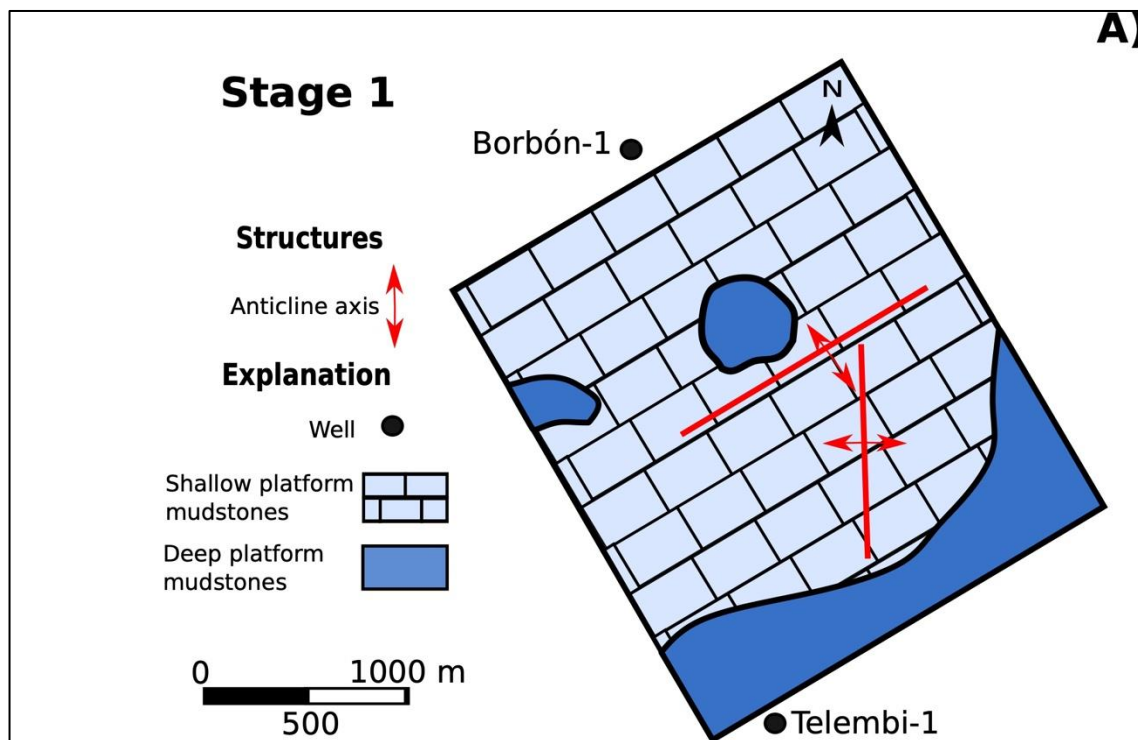


Figure 16. Paleogeographic maps of the study area for the proposed tectono-sedimentary stages. A) Stage 1: Representation of limestones on shallow marine platform and mudstones in deep marine platform during Late Cretaceous to Early Oligocene; B) Stage 2: Representation of sandstone on shallow platform and mudstone on deep platform during Early to Late Oligocene; C) Stage 3: Representation of sandstone in the paleo-valley and mudstone on deep, and shallow platform Late Oligocene to Late Miocene.

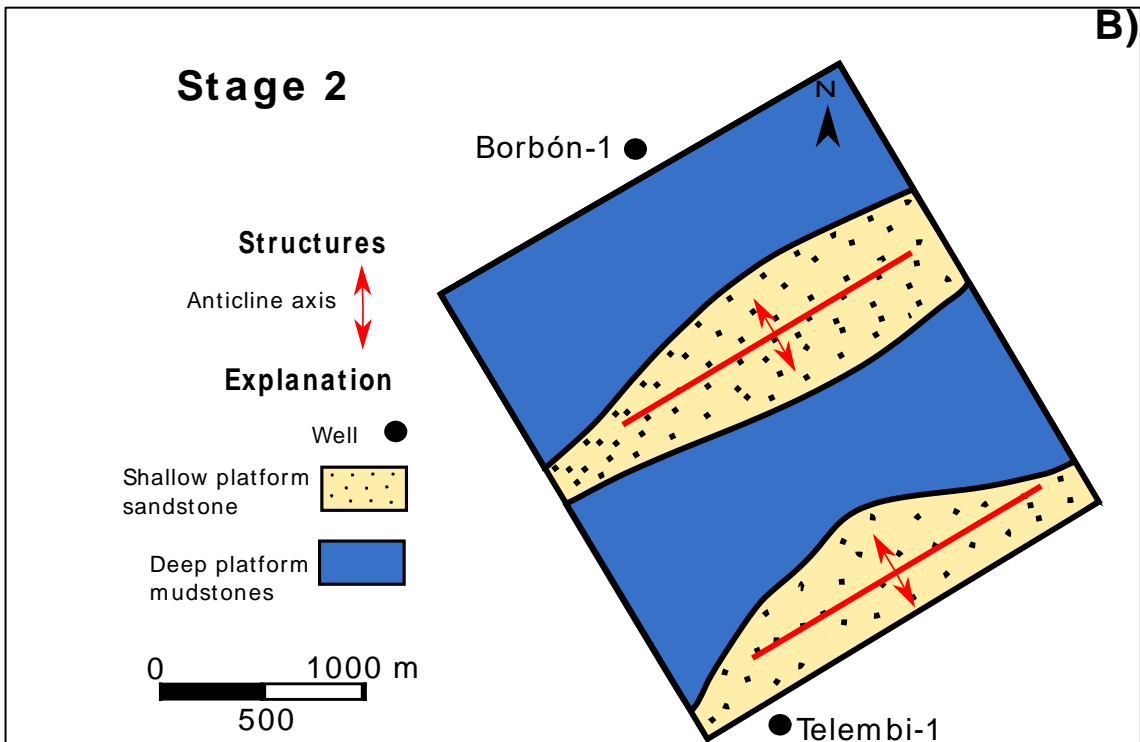


Figure 16. Continued

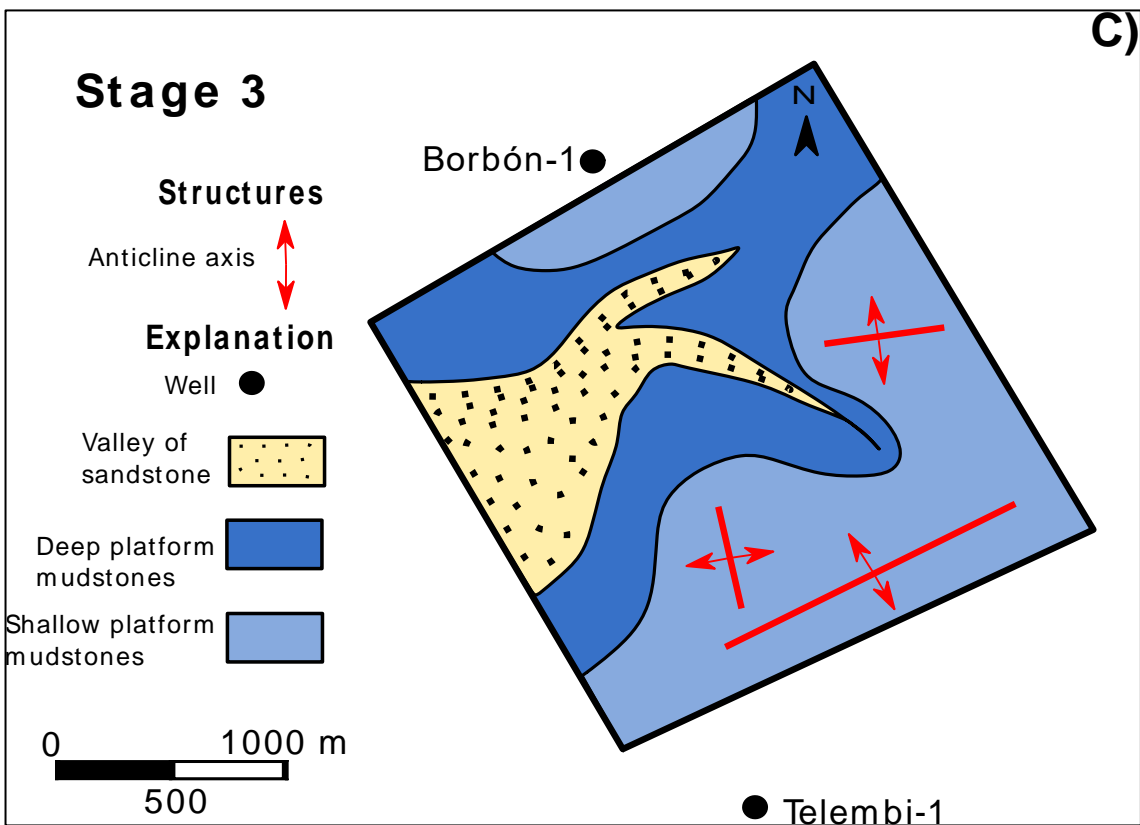


Figure 16. Continued

CHAPTER 6: CONCLUSION

- 1) A selected study area, located in the Esmeraldas-Borbón Basin (northern Ecuadorian forearc), is mainly characterized by compressional structures, such as anticlinal folds (structural high) and structural depression. These structures are affecting a Late Cretaceous to Neogene succession which is divided in eight depositional sequences. Based on thickness distribution of groups of sequences it is interpreted that the deposition between Late Cretaceous to Early Miocene was controlled by these structures.
- 2) A tectono-sedimentary evolution of the Esmeraldas-Borbón Basin is interpreted between Late Cretaceous and Early Miocene. This evolution consisted by the following three environments: 1) shallow to deep carbonatic platform, Late Cretaceous to Early Oligocene, with a southeast flow direction; 2) shallow to deep siliciclastic platform, Early to Late Oligocene, with a northeastern flow direction; and 3) platform to deep sea fan siliciclastic system, Late Oligocene to Late Miocene with northeastern flow direction.

References.

Bernal-Olaya, R., Mann, P., & Vargas, C. (2015). Earthquake, tomographic, seismic reflection, and gravity evidence for a shallowly dipping subduction zone beneath the Caribbean margin of northwestern Colombia. In C. Bartolini & P. Mann (Eds.), *Petroleum Geology and Potential of the Colombian Caribbean Margin*, AAPG Memoir (Vol. 108, pp. 247–270). Tulsa, OK: American Association of Petroleum Geologists. <https://doi.org/10.1306/13531939M1083642>

Brandes, C., & Winsemann, J. (2018). From incipient island arc to doubly-vergent orogen: A review of geodynamic models and sedimentary basin-fills of southern Central America. *Island Arc*, 27(5), 1–31. <https://doi.org/10.1111/iar.12255>

Campbell, K. A., Francis, D. A., Collins, M., Gregory, M. R., Nelson, C. S., Greinert, J., & Aharon, P. (2008). Hydrocarbon seep-carbonates of a Miocene forearc (East Coast Basin), North Island, New Zealand. *Sedimentary Geology*, 204(3–4), 83–105. <https://doi.org/10.1016/j.sedgeo.2008.01.002>

Daly, M. C. (1989). Correlations between Nazca/Farallon Plate kinematics and forearc basin evolution in Ecuador. *Tectonics*, 8(4), 769–790. <https://doi.org/10.1029/TC008i004p00769>

Deniaud, Y., Baby, P., Basile, C., Ordóñez, M., Mascle, G. H., & Montenegro, G. (1999). Neogene Evolution of the Main Ecuadorian Fore-arc Sedimentary Basins and Sediment Mass-Balance Inferences. 4th ISAG, Extended Abstracts, 201–205. http://horizon.documentation.ird.fr/exl-doc/pleins_textes/divers09-03/010022664.pdf

Jaillard, E., Lapierre, H., Ordoñez, M., Álava, J. T., Amórtegui, A., & Vanmelle, J. (2009). Accreted oceanic terranes in Ecuador: Southern edge of the Caribbean Plate? *Geological Society Special Publication*, 328, 469–485. <https://doi.org/10.1144/SP328.19>

Jaillard, E., Ordoñez, M., Benitez, S., Berrones, G., Jimenez, N., Montenegro, G., Zambrano, I., 1995. Basin development in an Accretionary, oceanic-floored fore-arc

setting: southern coastal Ecuador during Late Cretaceous-late Eocene time. AAPG Mem. 62, 615–631.

Jiménez, N., Ordóñez, M., & Montenegro, G. (2007). Bioestratigrafía De Las Formaciones Viche Y Angostura Del Neógeno De La Cuenca Esmeraldas , Ecuador : (2007). 229–234.

Kerr, A. C., Aspden, J. A., Tarney, J., & Pilatasig, L. F. (2002). The nature and provenance of accreted oceanic terranes in western Ecuador: Geochemical and tectonic constraints. *Journal of the Geological Society*, 159(5), 577–594.
<https://doi.org/10.1144/0016-764901-151>

Kerr, A. C. 2014. Oceanic plateaus. In: Rudnick, R. (ed.), *The Crust*. Chapter 18. *Treatise on Geochemistry*, 2nd edn (Holland, H. C., and Turekian, K. (Series eds.)). Elsevier, Amsterdam, Vol. 4, pp. 631–667.

Kerr, A. C., Aspden, J. A., Tarney, J., & Pilatasig, L. F. (2002). The nature and provenance of accreted oceanic terranes in western Ecuador: Geochemical and tectonic constraints. *Journal of the Geological Society*, 159(5), 577–594.
<https://doi.org/10.1144/0016-764901-151>

Lute, R., Gaedicke, C., Berglar, K., Schloemer, S., Franke, D., & Djajadihardja, Y. S. (2011). Petroleum systems of the Simeulue fore-arc basin, offshore Sumatra, Indonesia. *AAPG Bulletin*, 95(9), 1589–1616. <https://doi.org/10.1306/01191110090>

López, E. (2009). Evolution tectono-stratigraphique du double bassin avant - arc de la marge convergente Sud Colombienne – Nord Equatorienne pendant le Cénozoïque. *GeoAzur*, 349.

Mantilla, A. M., Jentszsch, G., Kley, J., & Alfonso-Pava, C. (2009). Configuration of the Colombian Caribbean Margin: Constraints from 2D Seismic Reflection Data and Potential Fields Interpretation, *Subduction Zone Geodynamics* (pp. 247–271). Dubai: Springer.

McNeill, L. C., Goldfinger, C., Kulm, L. D., & Yeats, R. S. (2000). Tectonics of the Neogene Cascadia forearc basin: Investigations of a deformed late Miocene unconformity. *Geological Society of America Bulletin*, 112(8), 1209–1224. [https://doi.org/10.1130/0016-7606\(2000\)112<1209:TOTNCF>2.0.CO;2](https://doi.org/10.1130/0016-7606(2000)112<1209:TOTNCF>2.0.CO;2)

Macias, K., 2018. Geoquímica de los Plutones de Pascuales y de Bajo Grande (Cantón Jipijapa): dataciones U-Pb en zircones e implicaciones geodinámicas. Eng Thesis, Universidad de Guayaquil, Ecuador. 117 pp.

Marcaillou, B., & Collot, J. Y. (2008). Chronostratigraphy and tectonic deformation of the North Ecuadorian-South Colombian offshore Manglares forearc basin. *Marine Geology*, 255(1–2), 30–44. <https://doi.org/10.1016/j.margeo.2008.07.003>

Matsumoto, R., Ryu, B.J., Lee, S.R., Lin, S., Wu, S., Sain, K., Pecher, I., and Riedel, M., (2011). Occurrence and exploration of gas hydrate in the marginal seas and continental margin of the Asia and Oceania region: *Marine and Petroleum Geology*, v. 28, no. 10, p. 1751–1767, doi: 10.1016/j.marpetgeo.2011.09.009.

Michaud, F., Proust, J.N., Collot, J.Y., Lebrun, J.F., Witt, C., Ratzov, G., Calderon, M. (2015). Quaternary sedimentation and active faulting along the Ecuadorian shelf: preliminary results of the ATACAMES Cruise (2012). *Marine Geophysical Research*, 36(1), 81–98. <https://doi.org/10.1007/s11001-014-9231-y>.

Noda, A. (2016). Forearc basins: Types, geometries, and relationships to subduction zone dynamics. *Bulletin of the Geological Society of America*, 128(5–6), 879–895. <https://doi.org/10.1130/B31345.1>

Ordoñez, M., Jimenez, N., Suarez, J. (2006) . Micropaleontología ecuatoriana : datos bioestratigráficos y paleoecológicos de las cuencas : Graben de Jambell Progreso . Manabi , Esmeraldas y Oriente , del levantamiento de la Peninsula de Santa Elena y de las cordilleras Chongon Colonche costera y occidental 634 p . 11

Ramírez, M.F. (2013). Undergraduate thesis. Registros de la deformación y del volcanismo en el dominio del antearco ecuatoriano: sedimentología y bioestratigrafía de la Formación Borbón. Faculty of Engineering in Earth Sciences, ESPOL. Guayaquil.

Vallejo, C., Spikings, R.A., Winkler, W., Luzieux, L., Chew, D., Page, L., (2006). The early interaction between the Caribbean plateau and the NW South American plate. *Terra Nova* 18, 264–269.

Van Melle, J., Vilema, W., Faure-Brac, B., Ordoñez, M., Lapierre, H., Jimenez, N., Jaillard, E., & Garcia, M. (2008). Pre-collision evolution of the Piñón oceanic terrane of SW Ecuador: Stratigraphy and geochemistry of the “Calentura Formation.” *Bulletin de La Societe Geologique de France*, 179(5), 433–443.
<https://doi.org/10.2113/gssgfbull.179.5.433>

Wells, R.E., Blakely, R.J., Sugiyama, Y., Scholl, D.W., and Dinterman, P.A., (2003) Basin-centered asperities in great subduction zone earthquakes: A link between slip, subsidence, and subduction erosion?: *Journal of Geophysical Research*, v. 108, no. B10, 2507, doi:10.1029/2002JB002072.